

## The deubiquitinase USP9X regulates FBW7 stability and suppresses colorectal cancer

Omar M. Khan, ... , Stephen A. Wood, Axel Behrens

*J Clin Invest.* 2018. <https://doi.org/10.1172/JCI97325>.

Research Article In-Press Preview Cell biology Gastroenterology

The tumor suppressor FBW7 targets oncoproteins such as c-MYC for ubiquitylation and is mutated in several human cancers. We noted that in a significant percentage of colon cancers, FBW7 protein is undetectable despite the presence of *FBW7* mRNA. To understand the molecular mechanism of FBW7 regulation in these cancers, we employed proteomics and identified the deubiquitinase USP9X as an FBW7 interactor. USP9X antagonised FBW7 ubiquitylation, and *Usp9x* deletion caused Fbw7 destabilization. Mice lacking *Usp9x* in the gut showed reduced secretory cell differentiation and increased progenitor proliferation, phenocopying *Fbw7* loss. In addition, *Usp9x* inactivation impaired intestinal regeneration and increased tumor burden in colitis-associated intestinal cancer. *c-Myc* heterozygosity abrogated increased progenitor proliferation and tumor burden in *Usp9x*-deficient mice, suggesting that *Usp9x* suppresses tumor formation by regulating Fbw7 protein stability and thereby reducing c-Myc. Thus, we identify a novel tumor suppressor mechanism in the mammalian intestine that arises from the posttranslational regulation of FBW7 by USP9X independent of somatic *FBW7* mutations.

Find the latest version:

<https://jci.me/97325/pdf>



# **The deubiquitinase USP9X regulates FBW7 stability and suppresses colorectal cancer**

Omar M. Khan<sup>1</sup>, Joana Carvalho<sup>2</sup>, Bradley Spencer-Dene<sup>2</sup>, Richard Mitter<sup>3</sup>, David Frith<sup>4</sup>, Ambrosius P. Snijders<sup>4</sup>, Stephen A. Wood<sup>5</sup>, and Axel Behrens<sup>1,6\*</sup>

<sup>1</sup>Adult Stem Cell Laboratory,

<sup>2</sup>Experimental Histopathology,

<sup>3</sup>Bioinformatics and Biostatistics, &

<sup>4</sup>Proteomics,

The Francis Crick Institute,

1 Midland Road,

London NW1 1AT

U.K.

<sup>5</sup>Griffith Institute for Drug Discovery,

Griffith University, Nathan,

Queensland 4111,

Australia.

<sup>6</sup>King's College London,

Faculty of Life Sciences and Medicine,

Guy's Campus,

London SE1 1UL,

U.K.

**\*Corresponding author:** Axel Behrens, Adult Stem Cell Laboratory, The Francis Crick Institute, 1 Midland Road, London NW1 1AT, U.K. Tel: +44 203 7961 194  
Email: axel.behrens@crick.ac.uk

**Conflict of interest statement:** The authors have declared that no conflict of interest exists.

**Licensing:** The Francis Crick Institute receives its core funding from Cancer Research UK, the UK Medical Research Council, and the Wellcome Trust, and therefore requires a Creative Commons CC-BY license in order to support publication fees for this manuscript.

## ABSTRACT

The tumor suppressor FBW7 targets oncoproteins such as c-MYC for ubiquitylation and is mutated in several human cancers. We noted that in a significant percentage of colon cancers, FBW7 protein is undetectable despite the presence of *FBW7* mRNA. To understand the molecular mechanism of FBW7 regulation in these cancers, we employed proteomics and identified the deubiquitinase USP9X as an FBW7 interactor. USP9X antagonised FBW7 ubiquitylation, and *Usp9x* deletion caused Fbw7 destabilization. Mice lacking *Usp9x* in the gut showed reduced secretory cell differentiation and increased progenitor proliferation, phenocopying *Fbw7* loss. In addition, *Usp9x* inactivation impaired intestinal regeneration and increased tumor burden in colitis-associated intestinal cancer. *c-Myc* heterozygosity abrogated increased progenitor proliferation and tumor burden in *Usp9x*-deficient mice, suggesting that Usp9x suppresses tumor formation by regulating Fbw7 protein stability and thereby reducing c-Myc. Thus, we identify a novel tumor suppressor mechanism in the mammalian intestine that arises from the posttranslational regulation of FBW7 by USP9X independent of somatic *FBW7* mutations.

## Introduction

The mammalian intestine is composed of repetitive differentiated and stem cell units called villi and crypts respectively. Stem cells are located at the bottom of crypts where they produce highly proliferating transit amplifying (TA) cells. TA cells differentiate into absorptive and secretory cells, the two main intestinal lineages. The absorptive lineage comprises enterocytes while the secretory lineage is composed of goblet (mucin-secreting), enteroendocrine (serotonin-secreting), and Paneth cells (that produce lysozyme) (1). Pathways including Wnt and Notch signaling (2) regulate the proliferation and differentiation of the mammalian gut epithelium. Wnt ligands activate  $\beta$ -catenin and increase expression of Wnt/TCF target genes (3), including *c-Myc*, which is required for stem cell maintenance (2). Notch signaling is active both in stem cells and in TA cells where it controls cell fate decisions (4).

The importance of Wnt signaling in gut homeostasis is highlighted by the recurring mutations of the adenomatous polyposis coli (*APC*) gene (5), encoding a negative regulator of Wnt signaling, in human colorectal cancers (CRCs). APC inhibits Wnt signaling by forming a cytosolic destruction complex with GSK3 $\beta$  and AXIN to allow E3 ubiquitin ligase-mediated proteasomal degradation of  $\beta$ -catenin (2). Mutant APC fails to target  $\beta$ -catenin for proteasomal degradation and thus results in increased downstream Wnt signaling, including increased *c-Myc* expression. *c-Myc* is the main mediator of Wnt/ $\beta$ -catenin function in CRC (6), and is required for formation of intestinal polyps in *Apc*<sup>min/+</sup> mice (7).

In addition to somatic *APC* mutations, chronic inflammatory conditions including Crohn's disease and ulcerative colitis also predispose patients to CRC (8, 9). Although mechanisms linking inflammatory colitis to CRC are incompletely understood, these cancers may also show activation of Wnt signaling, including activating  $\beta$ -catenin mutations (10), or amplification of *c-MYC* (11).

The tumor suppressor FBW7 functions as the substrate recognition component of an SCF (SKP1, CUL1 & F-box protein)-type E3-ubiquitin ligase complex (12) targeting several oncoproteins, including *c-MYC*, NICD1 and *c-JUN* for degradation



(13-22). These proteins have well-defined roles in gut homeostasis and CRC (23-25), and their accumulation induces overproliferation and impaired differentiation of the intestinal epithelium. Consistent with this function, *FBW7* is one of the most frequently mutated genes in human CRC, altered in approximately 10% of tumors (26, 27), and *Fbw7* inactivation accelerates tumorigenesis in *Apc<sup>min/+</sup>* mice (13, 28).

Enzymes counteracting the E3 ligases are the deubiquitinases (DUBs), which act by cleaving the ubiquitin chains off the substrate protein leading to either protein stabilization or change in its activity (29). Emerging evidence suggests that DUBs are also required for the maintenance of tissue homeostasis. For example, we previously showed that Usp28 deubiquitylates some Fbw7 substrates, thereby regulating murine gut homeostasis (30). In addition, Usp22 promotes CRC by stabilizing cyclin B1 (31). Thus, deregulation of either ubiquitylation or deubiquitylation may result in cancer.

The mechanism of tumor suppression by FBW7 has been intensively studied, and many relevant SCF(FBW7) substrates have been identified. However, the mechanisms controlling FBW7 function are relatively understudied. Here we report that FBW7 protein is consistently downregulated in human colorectal cancer and identify the deubiquitinase USP9X as a positive regulator of FBW7 stability. USP9X directly bound FBW7 and antagonised its ubiquitylation and proteasomal degradation. In murine gut, this positive regulation was required for maintenance of tissue homeostasis mainly via suppression of c-Myc and Notch1 proteins. Colitis-driven tumor formation was greatly accelerated in mice with intestine-specific deletion of *Usp9x*. Using genetic rescue experiments, we show that the increased tumor burden in *Usp9x*-deficient colon was mainly mediated by c-Myc accumulation. In addition, we find a strong correlation between USP9X and FBW7 immunohistochemical staining in human CRC and show that reduced USP9X was strongly associated with poor clinical outcome in those cancers.

## Results

### **FBW7 protein is low or absent in most human colorectal cancers**

To investigate the prevalence of altered post-transcriptional regulation of FBW7 protein in human CRC, we performed in situ hybridization (RNAscope) and immunohistochemistry (IHC) for FBW7 on serial sections from human tissue microarrays (TMAs) of CRC patients. A control RNA probe, for *PPIB* (cyclophilin-B), was clearly detected in all examined cases, confirming the presence of intact mRNA on individual TMA cores (Figure 1A). In contrast, *FBW7* mRNA levels differed greatly between samples. Whereas 50% of cases showed high *FBW7* mRNA signal, in the other half of cases *FBW7* mRNA was low or undetectable (Figure 1A and 1B).

The majority of *FBW7* low mRNA cases (with one exception) had undetectable or weak FBW7 immunostaining (Figure 1A, case #1), as expected. Intriguingly, most samples (11 of 14, 78.5 %) with *FBW7* high mRNA levels had weak to undetectable while only few (3 out of 14, 21.5%) had strong FBW7 immunostaining (Figure 1A, cases #2 & #3, and Figure 1C). Thus, altered transcriptional as well as post-transcriptional mechanisms result in restricted FBW7 levels in most (24 of 28, 86%) of the human colorectal cancers analyzed.

### **Identification of USP9X as an FBW7 binding partner**

To understand the molecular mechanism underlying FBW7 regulation at the protein level, we decided to determine the FBW7 interactome in human cells. For this, we immunoprecipitated (IP) endogenous FBW7 (using an FBW7 $\alpha$  specific antibody) from HEK293 cells and performed mass-spectrometric (MS) analysis of the eluted samples. In addition to the bait, FBW7, the top ranked proteins of the MS analysis included components of the SCF-type E3-ubiquitin ligase complex including SKP1 and several known SCF(FBW7) substrates including c-JUN, mTOR, and DEK (Supplementary Figure 1A and Supplementary Table). We also identified the deubiquitinase USP9X enriched in the FBW7 IP-elutes. Based on its tissue-specific

roles both in tumor promotion (32) and suppression (33), we focussed on USP9X for further validation and biochemical evaluation. First, we confirmed the interaction between endogenous FBW7 and USP9X by immunoprecipitation of FBW7 followed by western blots (Figure 1D–1F). Conversely, USP9X overexpressed in HEK293 cells pulled down endogenous FBW7 (Figure 1E). Second, to check whether USP9X interacted with other isoforms of FBW7 we overexpressed Flag-tagged FBW7  $\alpha$ ,  $\beta$  and  $\gamma$  respectively in HEK293 cells and confirmed USP9X interaction with  $\alpha$  and  $\beta$  isoforms but not with FBW7 $\gamma$  (Figure 1G).

### **USP9X counteracts FBW7 ubiquitylation**

Next, we investigated the biochemical significance of the FBW7-USP9X interaction. If USP9X were an FBW7 substrate, short-hairpin RNA (shRNA)-mediated knockdown of *FBW7* should result in USP9X stabilization. However, shRNA-mediated knockdown of *FBW7* had no effect on USP9X levels (Supplementary Figure 1B). Conversely, multiple different shRNAs targeting *USP9X* caused a sharp decrease in endogenous FBW7 whereas RBX1 and SKP1 protein levels, and *FBW7* mRNA were unaffected (Figure 2A and 2B). These results suggest that USP9X may control FBW7 protein stability and that FBW7 could be a USP9X substrate.

If USP9X-FBW7 interaction were to regulate FBW7 protein stability by reducing its proteasomal degradation then the proteasome inhibitor (MG132) should restore the levels of FBW7 in *USP9X*-silenced cells. Indeed, levels of Flag-FBW7 $\alpha$  and Flag-FBW7 $\beta$  were restored by MG132 in *USP9X*-silenced cells (Figure 2C and Supplementary Figure 1C). In addition, *USP9X* depletion resulted in a striking reduction in Flag-FBW7 $\alpha$  protein stability as judged by a cycloheximide time course experiment (Figure 2D and 2E).

To further understand FBW7 regulation by USP9X, we performed Ni-NTA pulldowns on lysates from HEK293 cells co-transfected with 6x-His-ubiquitin, Flag-FBW7 $\alpha$  and a scrambled (control) shRNA or a combination of two shRNAs targeting

*USP9X* (shU9#3+4). Knockdown of *USP9X* increased Flag-FBW7 $\alpha$  ubiquitylation (Figure 2F). Conversely, addition of recombinant GST-*USP9X* on eluted HA-ubiquitylated Flag-FBW7 $\alpha$  reduced FBW7 ubiquitylation in vitro but only had a negligible effect on eluted HA-ubiquitylated Flag-c-JUN, confirming substrate specificity of *USP9X* for FBW7 (Figure 2G and Supplementary Figure 2A).

FBW7 protein levels are regulated by proteasomal degradation (34), suggesting that FBW7 $\alpha$  is polyubiquitylated via Lys-48 (K48) linkage. To formally demonstrate this, we performed a Ubiquitin Chain Restriction analysis (Ubi-CRest) using purified polyubiquitylated Flag-FBW7 $\alpha$  as a substrate for K48- and K63-specific deubiquitinases (OTUBAIN 1 and AMSH, respectively), and *USP9X*. The high molecular weight species appearing in Flag-FBW7 western blots were indeed polyubiquitylated FBW7 $\alpha$  since a promiscuous DUB USP2 cleaved all the conjugated ubiquitins off FBW7 (Supplementary Figure 2B and 2C). In addition, only OTB1 and *USP9X*, but not AMSH, cleaved conjugated ubiquitins off FBW7 $\alpha$ , suggesting that the majority of polyubiquitylated FBW7 $\alpha$  is linked via K48. This was confirmed using a K48 linkage-specific antibody (Supplementary Figure 2C).

Flag-FBW7 $\alpha$  was stabilized by wild-type mUsp9x (V5-Usp9x) (Figure 2H) but not by a V5-C1566S catalytically dead mutant (Figure 2I). Additionally, mUsp9x expression greatly reduced ubiquitylation of Flag-FBW7 $\alpha$  whereas the catalytically dead mutant V5-C1566S slightly increased FBW7 ubiquitylation, perhaps indicating a dominant negative effect (Figure 2J). Thus *USP9X* DUB activity antagonises degradative K48-linked FBW7 polyubiquitylation.

### ***USP9X* negatively regulates SCF(FBW7) substrates**

Next, we examined the effect of *USP9X* loss on SCF(FBW7) substrates. Knockdown of *USP9X* using two different shRNAs caused a sharp decrease in endogenous FBW7 and concomitantly stabilized the SCF(FBW7) substrates c-MYC, c-JUN and CyclinE in 293T and HCT116 cells (Figure 3A and Supplementary Figure 3). The protein levels of USP28, another deubiquitinase previously reported to

differentially regulate FBW7 stability (35), were unaffected by USP9X knockdown (Figure 3A). To investigate USP9X function in primary cells, we isolated mouse adult fibroblasts (MAFs) from *Usp9x*-flox/flox mice and treated them with either adeno-*GFP* (control) or adeno-*Cre* to induce recombination (*Cre*). In vitro deletion of *Usp9x* in MAFs resulted in a decrease in Fbw7 protein and accumulation of SCF(Fbw7) substrates (Figure 3B). The protein levels of Itch, an E3 ligase previously shown to be a USP9X substrate (36), were unaffected in these cells. In addition, shRNA-mediated *ITCH* knockdown, unlike *USP9X* knockdown, did not result in stabilization of SCF(FBW7) substrates (Figure 3C). To confirm the relevance of FBW7 in the regulation of SCF(FBW7) substrates by USP9X, we knocked down *USP9X* using two different shRNAs in HCT116-*FBW7*<sup>+/+</sup> and HCT116-*FBW7*<sup>Δ/Δ</sup> cells. Whereas *USP9X* knockdown increased NICD1, Cyclin E, c-MYC and c-JUN protein levels in HCT116-*FBW7*<sup>+/+</sup> cells, in HCT116-*FBW7*<sup>Δ/Δ</sup> cells the protein levels of these substrates were already increased, and were not further affected by *USP9X* knockdown (Figure 3D). These results suggest that USP9X controls the protein stability of SCF(FBW7) substrates by direct regulation of FBW7 protein.

Consistent with the notion that USP9X negatively regulates c-MYC protein stability, c-MYC ubiquitylation was reduced in *USP9X* knockdown cells with no effect on its mRNA (Figure 3E and 3F). In agreement with these findings, *USP9X* silencing using two different siRNAs increased c-MYC transcriptional activity in HCT116-*FBW7*<sup>+/+</sup> but not in HCT116-*FBW7*<sup>Δ/Δ</sup> cells, as judged by a dual luciferase c-MYC reporter assay (Figure 3G). Thus, USP9X negatively regulates c-MYC activity via direct stabilization of FBW7.

### **Usp9x controls tissue homeostasis in murine intestine**

To explore *Usp9x*-mediated Fbw7 regulation in vivo, we crossed *Usp9x*-flox mice with the gut-specific *Villin*-cre mouse and analyzed transverse sections of gut from the resulting *Usp9x*<sup>F/F</sup>-*Villin*-cre and *Usp9x*<sup>F/y</sup>-*Villin*-cre mice (*Usp9x*<sup>ΔG</sup> mice). IHC analyses revealed uniform expression of *Usp9x* throughout the crypts and villi in

the gut of the control mice, whereas no staining was detected in the intestinal epithelium of *Usp9x*<sup>ΔG</sup> mice (Figure 4A). Cellular analysis revealed a significant increase in proliferating cells in *Usp9x*<sup>ΔG</sup> small intestine crypts, evident from IHC following a BrdU pulse (Figure 4B) and from the increased numbers of MCM6<sup>+</sup> cells extending from the crypt-villus junction down to the crypt base (Supplementary Figure 4A). Similar results were obtained in colonic crypts from *Usp9x*<sup>ΔG</sup> mice (Supplementary Figure 3B). Goblet and Paneth cell numbers in *Usp9x*<sup>ΔG</sup> villi and crypts were reduced (Figures 4C and 4D), as observed in *Fbw7*-deficient murine intestine (28). However, numbers of CBCs, enteroendocrine cells and enterocytes were similar between WT and *Usp9x*<sup>ΔG</sup> mice as judged by in situ hybridization of *Olfm4*, and chromogranin and alkaline phosphatase staining (Supplementary Figures 4C–E). There was a striking reduction in Fbw7 protein, while *Fbw7* mRNA was unaffected (Figure 4E and Supplementary Figure 4F), which was accompanied by c-Myc and c-Jun accumulation in *Usp9x*<sup>ΔG</sup> crypts (Figure 4E).

To establish which SCF(Fbw7) substrates mediate hyper-proliferation of TA cells and reduced secretory cell differentiation in *Usp9x*<sup>ΔG</sup> crypts, we crossed either *c-Myc*-flox or *c-Jun*-flox mice with *Usp9x*<sup>ΔG</sup> mice and compared the proliferation and differentiation in the gut of the resulting *c-Myc*<sup>ΔG/+</sup>; *Usp9x*<sup>ΔG</sup> and *c-Jun*<sup>ΔG/+</sup>; *Usp9x*<sup>ΔG</sup> mice with *Usp9x*<sup>ΔG</sup> mice. Deletion of one *c-Myc*, but not one *c-Jun* allele was sufficient to reduce TA cell numbers to WT levels whereas neither *c-Myc* nor *c-Jun* heterozygosity had any effect on the goblet cell numbers in *Usp9x*<sup>ΔG</sup> intestine (Figure 4F and Supplementary Figure 5A). Instead, reduced differentiation of TA cells in *Usp9x*<sup>ΔG</sup> intestine was most likely a consequence of increased Notch activity (Figure 4G) since treating *Usp9x*<sup>ΔG</sup> mice with the  $\gamma$ -secretase inhibitor dibenzazepine (DBZ) restored the number of goblet cells even beyond WT levels, with no effect on TA cell proliferation (Figure 4H and Supplementary Figure 5B). Hence, *Usp9x* controls tissue homeostasis in the murine gut by negatively regulating c-Myc and Notch1, most likely via stabilization of Fbw7.

### **Usp9x is required for tissue regeneration after acute colitis**

To further explore the role of Usp9x in tissue maintenance, damage and repair we used a standard model of Dextran Sodium Sulfate (DSS)-induced acute colitis in mice (Figure 5A). We first tested the protein and mRNA levels of *Usp9x* and *Fbw7* in different disease phases of DSS-induced colitis. For this, we fed WT littermates with 2.5% DSS in drinking water for 7 days and analyzed tissues by WB and qRT-PCR at 0 (normal), 7 (disease peak) and 21 (recovery) days. Notably, Usp9x and Fbw7 protein levels were dramatically reduced during the peak phase of colitis (day 7) and were restored to normal levels at later stages (Figure 5B). Conversely c-Myc and Notch1 (NICD1) accumulated during the disease peak and were reduced when the tissue recovered (Figure 5B). Strikingly, *Usp9x* mRNA was reduced by around 50% during the disease peak whereas *Fbw7* mRNA was not significantly affected throughout the experiment (Figure 5C), suggesting that decreased Fbw7 protein levels in response to colitis are the consequence of reduced *Usp9x* expression.

After DSS-induced colitis, *Usp9x*<sup>ΔG</sup> mice showed reduced body weight (Figure 5D), suggesting impaired intestinal regeneration. IHC revealed highly proliferative, disorganised crypt structures in colon ulcers from those mice, and a substantial increase in BrdU-positive proliferating cells (Figure 5E and 5F). In contrast, the number of goblet cells generated after regeneration in the *Usp9x*<sup>ΔG</sup> intestine was low, most likely due to increased NICD1 protein levels (Figure 5E and 5F). Thus, Usp9x may control the response to injury in murine colon by orchestrating the protein levels of SCF(Fbw7) substrates to ensure the transition from regenerating progenitor to cell differentiation.

### **Usp9x suppresses colorectal cancer**

The regulation of Fbw7 by Usp9x and increased proliferation of colonic crypts after acute colitis in *Usp9x*<sup>ΔG</sup> mice prompted us to test the role of Usp9x in colitis-mediated colorectal cancer. In the azoxymethane (AOM)/DSS-induced colorectal cancer model (Figure 6A), *Usp9x*<sup>ΔG</sup> mice showed an almost threefold increase in

tumor burden, including increases in tumor number and tumor area compared with WT controls (Figures 6B-6D). Similar results were obtained with *Fbw7*<sup>ΔG/+</sup> mice (Figure 6B–6D). Both the *Usp9x*<sup>ΔG</sup> and *Fbw7*<sup>ΔG/+</sup> mice showed reduced bodyweight throughout the experimental period, suggestive of a more advanced disease (Supplementary Figure 6A and 6B). Fbw7 protein levels were reduced in *Usp9x*<sup>ΔG</sup> tumors with a concomitant increase in c-Myc and c-Jun, as judged by western blots (Figure 6E). To validate the role of c-Myc in AOM/DSS mediated tumorigenesis in *Usp9x*<sup>ΔG</sup> mice, we inactivated one *c-Myc* allele in *Usp9x*<sup>ΔG</sup> mice and compared the number of tumors in *c-Myc*<sup>ΔG/+</sup>; *Usp9x*<sup>ΔG</sup> with those of *Usp9x*<sup>ΔG</sup> mice. Indeed, *c-Myc* heterozygosity was sufficient to reduce the tumor burden to WT levels in *Usp9x*<sup>ΔG</sup> mice, with a clear reduction of c-Myc staining in *c-Myc*<sup>ΔG/+</sup>; *Usp9x*<sup>ΔG</sup> tumors (Figure 6F and 6G). Thus, negative regulation of c-Myc by Usp9x via direct stabilization of Fbw7 protects mice from colitis-mediated colorectal cancer.

### **Reduced USP9X strongly correlates with reduced FBW7 protein and poor prognosis in human cancers**

To test the relationship between USP9X and FBW7 in human cancers we stained serial sections of human colon cancer TMAs for USP9X and FBW7 (Figure 7A). Both USP9X and FBW7 were readily detected in adjacent normal tissue in all cases. In CRC tumor tissue, USP9X and FBW7 showed a strong correlation in staining intensity, with 72% showing concomitant downregulation (Figures 7A, case #1, and 7B). In a smaller percentage of cases, both FBW7 and USP9X were strongly expressed (Figure 7A, case #2, and 7B). The correlation between FBW7 and USP9X protein expression was also evident in a panel of 8 human CRC cancer cell lines. FBW7 was only detectable by western blot in cell lines with higher USP9X protein (Figure 7C). Interestingly, this correlation was lost in two cell lines which harbour a *USP9X* or *FBW7* mutation respectively, further confirming the positive regulation of FBW7 by USP9X (Figure 7C).



In support of its pro-tumorigenic effect in mice, we found that low *USP9X* expression was strongly associated with poor survival in human CRC (Figure 7D). Moreover, *USP9X* was mutated in a small percentage of CRC patients. Interestingly, concurrent *FBW7* mutations predominantly occur in females (Fisher's exact test,  $p$ -value = 0.01) and not in males, ( $p$ -value = 1) (Figure 7E), suggesting that incomplete *USP9X* inactivation caused by random X inactivation in females may favour a second genetic mutation in *FBW7* gene to fully inactivate the function of the USP9X–FBW7 axis. Taken together, these data support the notion that USP9X is a tumor suppressor in the intestine via positive regulation of FBW7.

## Discussion

*FBW7* is a haploinsufficient tumor suppressor gene (37) mutated in a wide variety of human cancers but mechanisms regulating *FBW7* protein stability and activity are largely unknown. In this study, we identify a novel mechanism of *FBW7* protein regulation by the deubiquitinase *USP9X*. *USP9X* antagonized *FBW7* ubiquitylation and protected mice from colorectal cancer. Importantly, reduced *USP9X* expression predicted poor survival in human cancers. Thus, *USP9X* functions “indirectly” as a tumor suppressor, by controlling the protein stability of *FBW7*.

*USP9X* is a C19-peptidase family protein with a known deubiquitinase activity (36). It cleaves both K48 and K63 mediated linkages. *USP9X* can have both pro- and anti-tumorigenic functions depending on tumor type. For example, it functions as an oncogene in multiple myeloma and lymphoma (32), however, it is a potent tumor suppressor in the pancreas (33). Our data demonstrate that in addition to the pancreas, *USP9X* is also a tumor suppressor in the intestine. Although the E3 ligase Itch was shown to mediate the anti-tumor effects of *USP9X* in the pancreas (33), our data demonstrate that *USP9X* can prevent intestinal cancer by directly regulating the stability of *FBW7* protein.

Our data indicate that regulation of *Fbw7* plays a major role in mediating the loss-of-*Usp9x* phenotype in the intestine. Indeed, *Fbw7* protein levels were dramatically low in isolated crypts from *Usp9x*<sup>ΔG</sup> mice (Figure 4E) and the reduced differentiation and increased proliferation in the gut of *Usp9x*<sup>ΔG</sup> mice resembles gut phenotypes of *FBW7*<sup>ΔG</sup> mice (28). Similar to *Fbw7*<sup>ΔG</sup> intestine, c-Myc and Notch1 appear to be the main mediators of the *Usp9x*<sup>ΔG</sup> phenotypes.

The positive regulation of *FBW7* by *USP9X* reinforces the importance of protein turnover and regulation in tissue homeostasis and cancer. The regulation of *FBW7* protein by the deubiquitinase activity of *USP9X* is a direct and rapid mechanism of transiently regulating *FBW7* protein levels and thus its activity. Additionally, this mechanism may allow control of *FBW7* stability in an isoform-

specific manner as USP9X interacts with FBW7 $\alpha$  and  $\beta$ , but not with FBW7 $\gamma$  (Figure 1G).

The regulation of Fbw7 by Usp9x also appears to be crucial during intestinal regeneration. Indeed, *Usp9x* was transcriptionally downregulated during the peak phase of colitis, and this resulted in a reduction of FBW7 protein levels with a concomitant increase in c-Myc and NICD1 (Figure 5B and 5C). Importantly, *Usp9x* mRNA levels were restored after recovery from colitis, and c-Myc and NICD1 returned to normal. As expected, *Usp9x*<sup>ΔG</sup> colonic ulcers after acute colitis were marked by increased proliferation and decreased secretory differentiation, most likely because the normalization of c-Myc and NICD1 protein is delayed in the absence of Usp9x, and the damaged intestine was “locked” in a proliferative state (Figure 5E). Thus, Usp9x may function as an “emergency switch” in the injured intestine, which allows high proliferation required during regeneration, and subsequently mediates the transition to differentiation by restoring the levels of Fbw7.

Importantly, the regulation of FBW7 by USP9X has implications in human intestinal cancer. We found that a substantial number of human CRC tumors express normal levels of *FBW7* mRNA, but FBW7 protein was either undetected or weakly expressed (Figure 1A). In these patients FBW7 function appears to be compromised regardless of *FBW7* mutations. Our data suggest USP9X to be an important mediator of FBW7 protein stability. Out of 56 patients with low FBW7 IHC staining, 49 had low USP9X protein levels (Figure 7B). The strong and direct correlation between USP9X and FBW7 in human CRC, together with our biochemical characterization of FBW7 as a USP9X substrate, strongly suggests a causal role for USP9X loss in intestinal tumorigenesis. Consistent with this idea, we found that low USP9X expression is strongly associated with poor survival in colon cancer (Figure 7D).

The incidence of CRC in males is higher than in females (38). One plausible explanation for this apparent gender bias is the presence of tumor suppressor genes on the X-chromosome which protect females from the effects of loss-of-function mutations (39). In agreement with this idea, we find that a significant percentage of

female, but not male, colon cancer patients with *USP9X* mutations also carry a concomitant *FBW7* mutation (Figure 7E). Because males have only one *USP9X* allele, this supports the notion that females may require an additional “hit” in *FBW7* gene to achieve a sufficient decrease in function of the USP9X-FBW7 axis. Thus, USP9X is a crucial regulator of FBW7 protein levels and function, and the degradation of FBW7 in the absence of USP9X is a previously unappreciated mechanism of tumor promotion.

## Methods

### RNA in situ hybridization for *FBW7*

RNAscope® was performed on human CRC TMAs (CO811, US Biomax) as recommended by the manufacturer (<https://acdbio.com/technical-support/user-manuals>). Briefly, target retrieval was performed for 15 minutes followed by RNAscope® Protease Plus incubation for 30 minutes on the FFPE Sample Preparation. The counterstaining and mounting of the slides was performed on Tissue-Tek® Prisma™ staining machine.

### Mass spectrometry

Sub confluent HEK293 cells were treated with a proteasome inhibitor (MG132) for six hours. Cells were washed with ice-cold PBS and lysed in 1x Cell lysis buffer (CLB; Cell Signaling Technology, #9803) supplemented with protease inhibitors, PMSF (1 mM), and Sodium fluoride (5 mM). FBW7 $\alpha$  was immunoprecipitated with 5  $\mu$ g/ml of FBW7 $\alpha$  antibody (Bethyl Laboratories, A301-720A). Rabbit-IgG at 5  $\mu$ g/ml was used as a negative control. Immunoprecipitated complexes were washed 5 times in 1x ice-cold CLB. Eluted samples were run on 12 % Tris-HCL gel for 5 to 10 minutes at 150 volts. Gels were washed with distilled water, fixed, coomassie stained, and recovered in distilled water. Sample bands were diced with sterile razor blade on a glass slide pre-washed with 100% methanol and stored in distilled water for MS analyses as previously described (40).

### Source of cell lines

HEK293, HCT116-*FBW7*<sup>+/+</sup> and HCT116-*FBW7* <sup>$\Delta/\Delta$</sup> , COL205, HT29, HCT115, SW620, SW480, SW837 and SNUC1 cell lines were obtained from Cell Services at the Francis Crick Institute.

## **Western Blot Analysis and Quantitative RT-PCR**

Immunoblots were carried out as previously described (28). Antibodies against USP9X (Bethyl Laboratories, A301-351A) , FBW7 $\alpha$  (Bethyl Laboratories, A301-720), c-Jun (BD Biosciences, #610326), active Notch-1 (Abcam, ab8925), c-Myc, Cyclin-E (Santa Cruz, sc-788 & sc-481),  $\alpha$ -Tubulin (Abcam, ab7291), Apu2 clone, K48-linkage (Millipore, #05-1307) and  $\beta$ -Actin (Sigma, A3854) were used.

For qRT-PCR analysis, total mRNA was isolated from dissected ileum as previously described (28). Results normalized to  $\beta$ -actin were presented as fold induction over control. The primers used for qRT-PCR analysis were previously published (24, 28, 33).

## **Ubiquitylation Assays**

HEK293 cells were co-overexpressed with 6x-His-ubiquitin along with Flag-FBW7 and a control or *USP9X* specific shRNA (shU9 3+4). 48 h after transfection, cells were treated with MG132 for 6 hours, washed, collected and lysed in Buffer A (6M guanidium hydrochloride, 0.1 M Na<sub>2</sub>HPO<sub>4</sub>, and 0.1 M NaH<sub>2</sub>PO<sub>4</sub>) supplemented with 20 mM imidazole. The ubiquitylated proteins were precipitated using Nickel-NTA beads for 2 hours at room temperature, washed three times in Buffer A, twice in Buffer A/TI (1 volume Buffer A + 3 volume 25 mM Tris-HCL + 10 mM imidazole), and twice in Buffer TI (25 mM Tris-HCL + 10 mM imidazole). The bead-bound ubiquitylated proteins were eluted in 1M imidazole-containing sample buffer, resolved on 7.5 % Tris-HCL gel and transferred to nitrocellulose membranes. The blots were probed with Flag-HRP antibody (Sigma, A8592).

For in vitro deubiquitylation, Flag-FBW7 was co-overexpressed with HA-ubiquitin for 48 hours in HEK293 cells. The transfected cells were treated with MG132 as above and the ubiquitylated proteins were immunoprecipitated using anti-HA affinity agarose (Sigma, A7470) overnight. The bead-bound HA-ubiquitylated complexes were washed once in 1X CLB and incubated with 0.5 mg/ml HA-peptide (Sigma, I2149) for 1 hour at 4°C with constant shaking. Flag-FBW7 was immunoprecipitated

from two sequentially pooled HA-peptide elutions using the Flag-M2 affinity beads (Sigma, F2426) for up to 4 hours at 4°C. The polyubiquitinated Flag-FBW7 bound M2-beads were then washed three times in PBS-Tween (0.05%) and eluted twice with 0.25 mg/ml Flag peptide (Sigma, F4799) in TNT-300 buffer (50 mM Tris pH 7.4, 300 mM NaCl, 1% TX-100). Pooled Flag eluates were then used for in vitro deubiquitylation experiments using either Ubiquitin Chain Restriction (UbiCRest) kit (Boston Biochem, K-400) or recombinant GST-USP9X (Boston Biochem, E-552). The reaction was performed in a final volume of 25 µl for 30 minutes at 37°C and stopped by adding 5 µl of 5X sample buffer and boiling the samples at 95°C for 5 minutes. The samples were resolved as above.

### **c-MYC transcriptional activity**

MYC transcriptional activity was determined in HCT116 cells using Cignal Myc Reporter Assay kit from SABiosciences (CCS-012L).

### **Mouse lines**

Mice carrying conditional alleles for *Usp9x* and *Fbw7* were previously described (16, 33). Similarly, *c-Jun*-flox and *Villin-Cre* mice were described before (41, 42). *c-Myc*-flox mice were a gift from Dinis Calado (The Francis Crick Institute, London, UK).

### **Histological analysis and quantifications**

Mice injected with 100 mg/kg BrdU (Sigma) intraperitoneally (i.p.) 2.5 hr prior to sacrifice were euthanized by cervical dislocation and the small intestines were dissected out. The intestines were cut longitudinally into pieces of similar size, opened and fixed overnight in 10 % neutral buffered formalin, briefly washed with PBS and transferred into 70% ethanol, roll processed and embedded into paraffin. Sections were cut at 4 µm for Haematoxylin & Eosin (H&E) staining, AB/PAS staining, immunohistochemistry (IHC) and immunofluorescence. Antibodies against

Usp9x (Bethyl Laboratories, A301-351), active-Notch1 (Abcam, ab8925), c-Myc (Santa Cruz, sc-788), and Lysozyme (DAKO, A0099) were used.

To quantify the average BrdU positive cells per crypt, 100 full crypts were scored from 3–8 mice per group. Goblet cells were quantified from 100 ileal villi from at least 5 mice per group. Paneth cells were quantified from 100 crypts from at least 5 mice per group.

### **Dibenzazepine (DBZ) treatment**

Six-to-eight-week-old mice were treated with 2 mg/kg body weight  $\gamma$ -secretase inhibitor (DBZ) (Tocris #4489), intraperitoneally for five consecutive days. All mice were injected with 100 mg/kg BrdU 4 hours after the final DBZ injection and culled two to three hours after BrdU injection. The gut rolls were prepared as described above.

### **DSS induced colitis**

Mice were fed with 2.5% DSS in drinking water for 7 days. At day 11 and/or 21, all mice were culled 2.5 h after 100 mg/kg body weight BrdU injection. Colons were washed in ice-cold PBS and fixed in 10% NBF overnight. Fixed tissues were processed for IHC as described above.

### **AOM/DSS induced colorectal cancer**

Mice were given a single intraperitoneal injection of 10 mg/kg body weight azoxymethane (AOM, Sigma). One week after AOM injection, mice were fed with 2.5% DSS in drinking water for another week. All mice were humanely killed either 12 weeks after AOM injection or when they showed signs of ill health.

### **Survival analysis**

The Cancer Genome Atlas (TCGA) RNASeqv2 RSEM gene abundance estimates for 382 colorectal adenocarcinoma patient tumor samples were downloaded from



cBioPortal (43, 44) and combined with patients' clinical information. Samples with missing overall survival status/time were removed from the analysis. Those remaining were stratified into either low or high USP9X expression groups based on a 2/3 split of the abundance scores for that gene. A Kaplan-Meier survival curve was generated and a log-rank test was used to determine the significance of the difference in overall survival due to the expression groups.

### **Mutational analysis of CRC cohorts**

Data for 831 exome-sequenced colorectal adenocarcinoma patient samples with corresponding gender information were downloaded from cBioPortal (42) to test for co-occurrence of *USP9X* and *FBW7* mutations using a Fisher's exact test. The samples were composed of two cohorts: TCGA dataset ( $n = 212$ ) and the Dana-Farber Cancer Institute's (DFCI) dataset ( $n = 619$ ) from references (6, 45).

### **Statistics**

Statistical analysis was carried out using GraphPad Prism software. 2-tailed Student's *t* tests were used to generate *P* values unless otherwise indicated. A *P* value of  $< 0.05$  was considered significant.

### **Study Approval**

Mouse experiments were carried out in accordance with UK Home Office guidelines, overseen by the Animal Welfare and Ethical Review Body at the Francis Crick Institute.

### **Author contributions**

A.B. and O.M.K. designed the experiments and wrote the manuscript. O.M.K. performed majority of experiments and analyzed the data. B.S. and D.F. performed the FBW7 mass-spectrometry experiment and analyzed the data. B.S.D and J.C. performed IHC and RNAscope. R.M. performed survival analysis. S.A.W. kindly

provided the *Usp9x*-conditional mouse.

## **Acknowledgements**

We are grateful to the BRF and Equipment Park at the Francis Crick Institute. We thank J. Nelson, R. Sancho and V. Li for critical reading of the manuscript. We would like to thank D. Calado for providing *c-Myc*-conditional mice. This work was supported by the Francis Crick Institute, which receives its core funding from Cancer Research UK (FC001039), the UK Medical Research Council (FC001039), and the Wellcome Trust (FC001039). O.M.K was supported by an EMBO long-term postdoctoral fellowship (ALTF 459-2013) and Swedish Research Councils' international postdoctoral fellowship (D0035901).

## Figure Legends

**Figure 1. FBW7 is downregulated in human CRC.** (A) Representative images of RNAscope for *PPIB* and *FBW7*, and FBW7 IHC on serial sections from human TMAs. u.d., undetected. Scale bar = 10 mm. (B) Quantification of *FBW7* mRNA on colorectal cancer TMAs in 28 tissue cores positive for a control *PPIB* mRNA. (C) Quantification of FBW7 IHC in tissue cores from A. (D–F) Endogenous FBW7 interacts with endogenous USP9X and USP9X interacts with endogenous FBW7 in HEK293 cells. Black line in D indicates noncontiguous lanes from the same gel. siFBW7 control in F confirms antibody specificity of FBW7 and represents a negative control for FBW7-USP9X interaction. (G) Endogenous USP9X interacts with epitope-tagged FBW7 isoforms  $\alpha$  and  $\beta$ .

**Figure 2. FBW7 is a USP9X substrate.** (A and B) USP9X knockdown using multiple shRNAs reduced FBW7 protein levels with no effect on its mRNA. (C) MG132 rescues reduced FBW7 protein levels in USP9X silenced cells. (D) USP9X knockdown reduced the half-life of FBW7 protein. (E) Quantification of 3 independent experiments performed as in D. (F) Increased ubiquitylation of FBW7 in USP9X-silenced cells, UM = unmodified. (G) *In vitro* deubiquitylation of FBW7 by recombinant GST-USP9X, UM = unmodified. (H and I) Western blots for Flag-FBW7 $\alpha$  in HEK293 cells co-overexpressing wildtype (V5-Usp9x) or catalytically dead (V5-C1566S) mouse Usp9x. (J) Western blots on Ni-NTA pulldown samples from cells co-transfected with Flag-FBW7 $\alpha$  and the indicated constructs, UM = unmodified. All experiments were done in HEK293 cells.

**Figure 3. USP9X negatively regulates SCF(FBW7) substrates.** (A) Accumulation of SCF(FBW7) substrates in *USP9X*-silenced HEK293 cells. (B) Accumulation of SCF(Fbw7) substrates in *Usp9x*-knockout murine adult fibroblasts. (C) Western blots showing levels of SCF(FBW7) substrates in *USP9X*- and *ITCH*-silenced HEK293 cells. (D) Accumulation of SCF(FBW7) substrates with *USP9X* silencing was abolished in HCT116-*FBW7*<sup>ΔΔ</sup> colorectal cancer cell line. (E and F) Western blots for ubiquitylated c-Myc on Ni-NTA pulldown from HEK293 cells overexpressing Flag-c-Myc and 6x-His-tagged ubiquitin and co-transfected with the indicated shRNAs. UM = unmodified. *c-MYC* mRNA levels in the same cells are shown in F. (G) c-MYC luciferase activity in HCT116 cells with indicated genotypes and siRNA treatments. Mean of 2 independent experiments shown.

**Figure 4. Usp9x controls intestinal tissue homeostasis.** (A, B, C, and D) Representative immunohistochemistry (IHC) sections for Usp9x (A), transit-amplifying cells (BrdU, B), goblet cells (AB/PAS, C), and Paneth cells (lysozyme, D), in wildtype (*Usp9x*<sup>+/+</sup>) and *Usp9x*-knockout mouse gut. Scale bars = 50 μm. Right panels, quantification from B–D, n = 5–8 mice/group. (E) Western blots for the indicated proteins in freshly isolated crypts from WT (wildtype) and *Usp9x*-knockout mouse gut. Black line indicates noncontiguous lanes from the same gel. (F) BrdU staining on gut cross sections from *Usp9x*<sup>ΔG</sup> mice. Scale bars = 50 μm. Right panel, quantification from F, n = 3–4 mice/group. (G) IHC for activated notch (NICD1) in mouse gut, scale bars = 50 μm. (H) AB/PAS staining on guts from indicated mice treated with a vehicle or a notch inhibitor (DBZ), scale bars = 50 μm. Right panel, quantification from H, n = 3–4 mice/group. Data are shown as mean + SD and statistical significance is calculated by student's t-test.

**Figure 5. *Usp9x* is required for tissue regeneration during acute colitis.** (A) Schematic of acute colitis protocol. (B) Western blots for the indicated proteins in six independent wildtype mice fed with (day 7, “peak” & day 21, “recovery”) or without (day 0, “normal”) 2.5 % DSS in water. (C) qRT-PCR analysis for *Usp9x* and *Fbw7* mRNA in different phases of colitis from experiment in B. Statistical significance calculated by one-way ANOVA. (D) Weight curves from DSS induced colitis experiment in indicated mice, n = 7–8/group. \* = p <0.05. (E) Representative IHC sections for H&E, BrdU, AB/PAS and NICD1 from *Usp9x*<sup>+/+</sup> and *Usp9x*<sup>ΔG</sup> mice. Scale bars = 100 μm. (F) Quantification of BrdU+ and AB/PAS+ cells from experiment in D. Data presented as mean, statistical significance calculated by student’s t-test in D and F.

**Figure 6. *Usp9x* suppresses colorectal cancer.** (A) Schematic of AOM/DSS induced colorectal cancer model. (B) H&E on sections from transformed colons of the indicated genotypes. Scale bars = 100 μm. (C) Number of tumors in each mouse from experiment in B, n = 5–13/group. (D) Tumor area represented as mm<sup>2</sup> in mice from B, n = 5–13/group. (E) Western blots showing levels of indicated proteins in four independent tumors from B. (F) H&E and c-Myc staining on sections from transformed colons of the indicated genotypes. Scale bars = 50 μm. (G) Average number of tumors in indicated mice from experiment in F, n = 3–5/group. Data presented as mean, statistical significance calculated by one-way ANOVA in C and D, and by student’s t-test in G.

**Figure 7. Reduced USP9X is associated with poor prognosis in human colorectal cancer.** (A) IHC for the indicated proteins on human colorectal cancer tissue microarrays, including associated normal tissue. Scale bars = 50 mm. (B) Quantification of staining intensities from sections in A, and their Spearman's rank correlation. (C) Western blots showing positive correlation of USP9X and FBW7 protein levels in 8 different colorectal cancer cell lines. Red = *USP9X* mutant, pink = *FBW7* truncation mutant (homozygous) cell lines respectively. Black line indicates noncontiguous lanes from the same gel. (D) Kaplan-Meier plot showing comparison of survival between *USP9X*-low and -high expression groups of colorectal cancer patients. Data are from TCGA. (E) Mutational status of *USP9X* and *FBW7* in CRC patients. Data are from the TCGA dataset of 212 patients and the DFC Colorectal Adenocarcinoma dataset of 619 patients published in refs<sup>(6,45)</sup>. Data viewed with cBioPortal. Only samples with alterations in either *USP9X* or *FBW7* are shown. Fisher's exact test  $p = 0.01$  for females and  $p = 1$  for males.

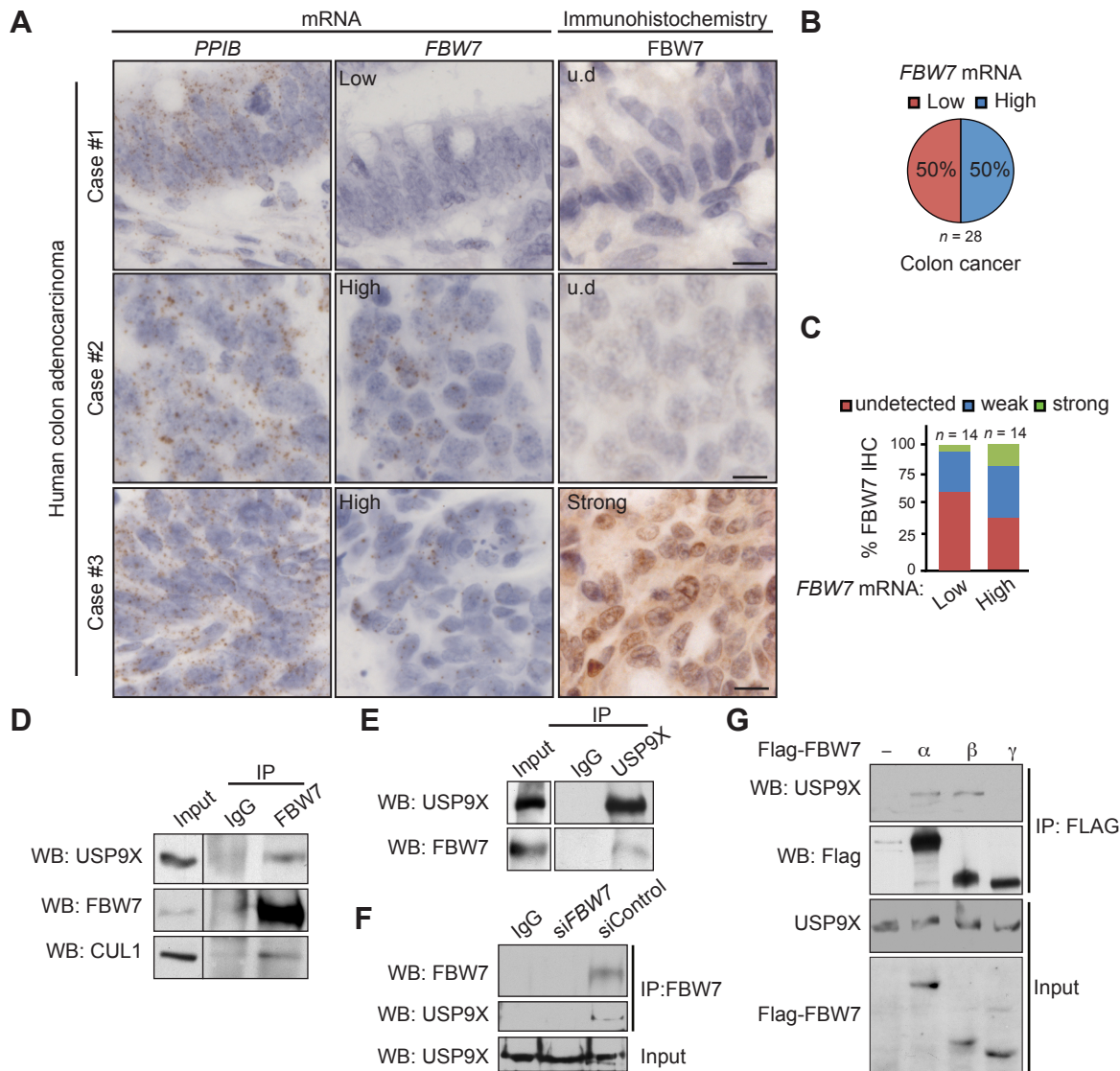
## References

1. Scoville DH, Sato T, He XC, and Li L. Current view: intestinal stem cells and signaling. *Gastroenterology*. 2008;134(3):849-64.
2. de Lau W, Barker N, and Clevers H. WNT signaling in the normal intestine and colorectal cancer. *Front Biosci*. 2007;12(471-91).
3. Clevers H. Wnt/beta-catenin signaling in development and disease. *Cell*. 2006;127(3):469-80.
4. Fre S, Huyghe M, Mourikis P, Robine S, Louvard D, and Artavanis-Tsakonas S. Notch signals control the fate of immature progenitor cells in the intestine. *Nature*. 2005;435(7044):964-8.
5. Kinzler KW, and Vogelstein B. Lessons from hereditary colorectal cancer. *Cell*. 1996;87(2):159-70.
6. Cancer Genome Atlas N. Comprehensive molecular characterization of human colon and rectal cancer. *Nature*. 2012;487(7407):330-7.
7. Sansom OJ, Meniel VS, Muncan V, Phesse TJ, Wilkins JA, Reed KR, Vass JK, Athineos D, Clevers H, and Clarke AR. Myc deletion rescues Apc deficiency in the small intestine. *Nature*. 2007;446(7136):676-9.
8. Ekblom A, Helmick C, Zack M, and Adami HO. Increased risk of large-bowel cancer in Crohn's disease with colonic involvement. *Lancet*. 1990;336(8711):357-9.
9. Ekblom A, Helmick C, Zack M, and Adami HO. Ulcerative colitis and colorectal cancer. A population-based study. *N Engl J Med*. 1990;323(18):1228-33.
10. Kohno H, Suzuki R, Sugie S, and Tanaka T. Beta-Catenin mutations in a mouse model of inflammation-related colon carcinogenesis induced by 1,2-dimethylhydrazine and dextran sodium sulfate. *Cancer Sci*. 2005;96(2):69-76.
11. Yaeger R, Shah MA, Miller VA, Kelsen JR, Wang K, Heins ZJ, Ross JS, He YT, Sanford E, Yantiss RK, et al. Genomic Alterations Observed in Colitis-Associated Cancers Are Distinct From Those Found in Sporadic Colorectal Cancers and Vary by Type of Inflammatory Bowel Disease. *Gastroenterology*. 2016;151(2):278-+.
12. Welcker M, and Clurman BE. FBW7 ubiquitin ligase: a tumour suppressor at the crossroads of cell division, growth and differentiation. *Nat Rev Cancer*. 2008;8(2):83-93.
13. Babaei-Jadidi R, Li N, Saadeddin A, Spencer-Dene B, Jandke A, Muhammad B, Ibrahim EE, Muraleedharan R, Abuzinadah M, Davis H, et al. FBXW7 influences murine intestinal homeostasis and cancer, targeting Notch, Jun, and DEK for degradation. *J Exp Med*. 2011;208(2):295-312.
14. Davis H, Lewis A, Behrens A, and Tomlinson I. Investigation of the atypical FBXW7 mutation spectrum in human tumours by conditional expression of a heterozygous propellor tip missense allele in the mouse intestines. *Gut*. 2013.
15. Flugel D, Gorlach A, and Kietzmann T. GSK-3beta regulates cell growth, migration, and angiogenesis via Fbw7 and USP28-dependent degradation of HIF-1alpha. *Blood*. 2012;119(5):1292-301.
16. Jandke A, Da Costa C, Sancho R, Nye E, Spencer-Dene B, and Behrens A. The F-box protein Fbw7 is required for cerebellar development. *Dev Biol*. 2011;358(1):201-12.

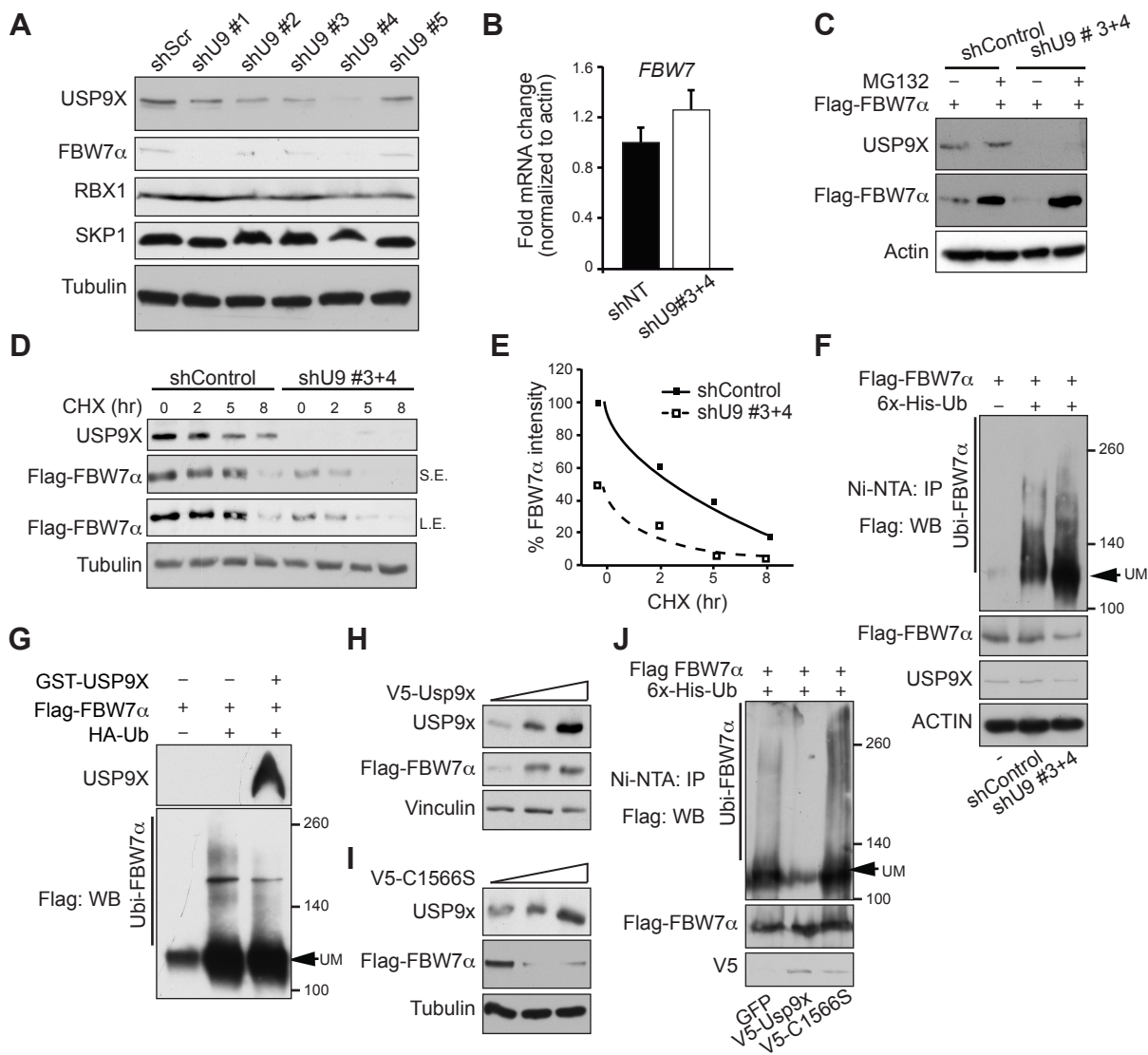
17. King B, Trimarchi T, Reavie L, Xu L, Mullenders J, Ntziachristos P, Aranda-Orgilles B, Perez-Garcia A, Shi J, Vakoc C, et al. The Ubiquitin Ligase FBXW7 Modulates Leukemia-Initiating Cell Activity by Regulating MYC Stability. *Cell*. 2013;153(7):1552-66.
18. Koepp DM, Schaefer LK, Ye X, Keyomarsi K, Chu C, Harper JW, and Elledge SJ. Phosphorylation-dependent ubiquitination of cyclin E by the SCFFbw7 ubiquitin ligase. *Science*. 2001;294(5540):173-7.
19. Matsumoto A, Tateishi Y, Onoyama I, Okita Y, Nakayama K, and Nakayama KI. Fbxw7beta resides in the endoplasmic reticulum membrane and protects cells from oxidative stress. *Cancer Sci*. 2011;102(4):749-55.
20. Nateri AS, Riera-Sans L, Da Costa C, and Behrens A. The ubiquitin ligase SCFFbw7 antagonizes apoptotic JNK signaling. *Science*. 2004;303(5662):1374-8.
21. Onoyama I, Suzuki A, Matsumoto A, Tomita K, Katagiri H, Oike Y, Nakayama K, and Nakayama KI. Fbxw7 regulates lipid metabolism and cell fate decisions in the mouse liver. *J Clin Invest*. 2011;121(1):342-54.
22. Popov N, Herold S, Llamazares M, Schulein C, and Eilers M. Fbw7 and Usp28 regulate myc protein stability in response to DNA damage. *Cell Cycle*. 2007;6(19):2327-31.
23. Riccio O, van Gijn ME, Bezdek AC, Pellegrinet L, van Es JH, Zimmer-Strobl U, Strobl LJ, Honjo T, Clevers H, and Radtke F. Loss of intestinal crypt progenitor cells owing to inactivation of both Notch1 and Notch2 is accompanied by derepression of CDK inhibitors p27Kip1 and p57Kip2. *EMBO Rep*. 2008;9(4):377-83.
24. Sancho R, Nateri AS, de Vinuesa AG, Aguilera C, Nye E, Spencer-Dene B, and Behrens A. JNK signalling modulates intestinal homeostasis and tumorigenesis in mice. *EMBO J*. 2009;28(13):1843-54.
25. Aguilera C, Nakagawa K, Sancho R, Chakraborty A, Hendrich B, and Behrens A. c-Jun N-terminal phosphorylation antagonises recruitment of the Mbd3/NuRD repressor complex. *Nature*. 2011;469(7329):231-5.
26. Sjoblom T, Jones S, Wood LD, Parsons DW, Lin J, Barber TD, Mandelker D, Leary RJ, Ptak J, Silliman N, et al. The consensus coding sequences of human breast and colorectal cancers. *Science*. 2006;314(5797):268-74.
27. Voutsadakis IA. The ubiquitin-proteasome system in colorectal cancer. *Biochim Biophys Acta*. 2008;1782(12):800-8.
28. Sancho R, Jandke A, Davis H, Diefenbacher ME, Tomlinson I, and Behrens A. F-box and WD repeat domain-containing 7 regulates intestinal cell lineage commitment and is a haploinsufficient tumor suppressor. *Gastroenterology*. 2010;139(3):929-41.
29. Komander D, Clague MJ, and Urbe S. Breaking the chains: structure and function of the deubiquitinases. *Nat Rev Mol Cell Biol*. 2009;10(8):550-63.
30. Diefenbacher ME, Chakraborty A, Blake SM, Mitter R, Popov N, Eilers M, and Behrens A. Usp28 counteracts Fbw7 in intestinal homeostasis and cancer. *Cancer Res*. 2015;75(7):1181-6.
31. Lin Z, Tan C, Qiu Q, Kong S, Yang H, Zhao F, Liu Z, Li J, Kong Q, Gao B, et al. Ubiquitin-specific protease 22 is a deubiquitinase of CCNB1. *Cell Discov*. 2015;1(
32. Schwickart M, Huang X, Lill JR, Liu J, Ferrando R, French DM, Maecker H, O'Rourke K, Bazan F, Eastham-Anderson J, et al. Deubiquitinase USP9X



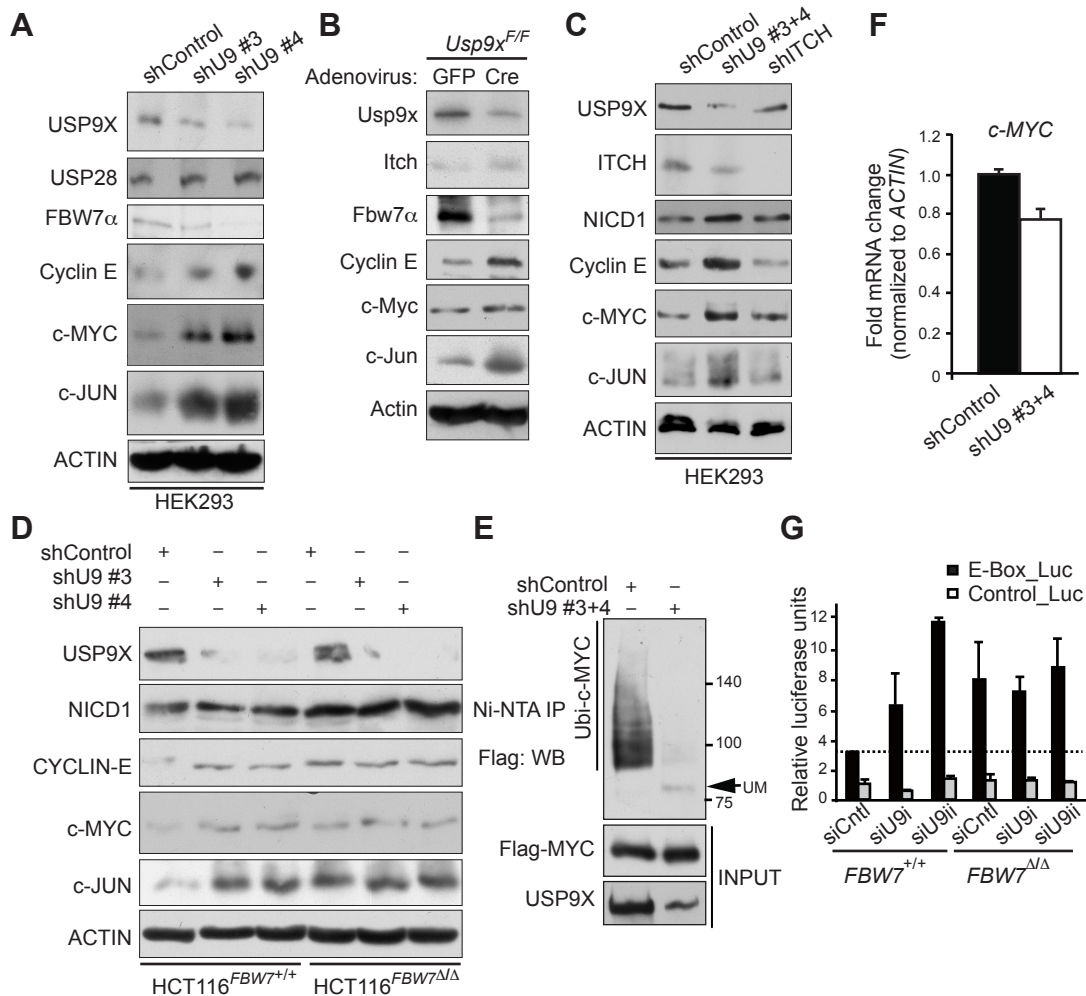
- stabilizes MCL1 and promotes tumour cell survival. *Nature*. 2010;463(7277):103-7.
33. Perez-Mancera PA, Rust AG, van der Weyden L, Kristiansen G, Li A, Sarver AL, Silverstein KA, Grutzmann R, Aust D, Rummele P, et al. The deubiquitinase USP9X suppresses pancreatic ductal adenocarcinoma. *Nature*. 2012;486(7402):266-70.
  34. Min SH, Lau AW, Lee TH, Inuzuka H, Wei S, Huang P, Shaik S, Lee DY, Finn G, Balastik M, et al. Negative regulation of the stability and tumor suppressor function of Fbw7 by the Pin1 prolyl isomerase. *Mol Cell*. 2012;46(6):771-83.
  35. Schulein-Volk C, Wolf E, Zhu J, Xu W, Taranets L, Hellmann A, Janicke LA, Diefenbacher ME, Behrens A, Eilers M, et al. Dual regulation of Fbw7 function and oncogenic transformation by Usp28. *Cell Rep*. 2014;9(3):1099-109.
  36. Mouchantaf R, Azakir BA, McPherson PS, Millard SM, Wood SA, and Angers A. The ubiquitin ligase itch is auto-ubiquitylated in vivo and in vitro but is protected from degradation by interacting with the deubiquitylating enzyme FAM/USP9X. *J Biol Chem*. 2006;281(50):38738-47.
  37. Mao JH, Perez-Losada J, Wu D, Delrosario R, Tsunematsu R, Nakayama KI, Brown K, Bryson S, and Balmain A. Fbxw7/Cdc4 is a p53-dependent, haploinsufficient tumour suppressor gene. *Nature*. 2004;432(7018):775-9.
  38. <http://www.cancerresearchuk.org/>. Bowel cancer incidence statistics.
  39. Dunford A, Weinstock DM, Savova V, Schumacher SE, Cleary JP, Yoda A, Sullivan TJ, Hess JM, Gimelbrant AA, Beroukheim R, et al. Tumor-suppressor genes that escape from X-inactivation contribute to cancer sex bias. *Nat Genet*. 2017;49(1):10-6.
  40. Schwanhauser B, Busse D, Li N, Dittmar G, Schuchhardt J, Wolf J, Chen W, and Selbach M. Global quantification of mammalian gene expression control. *Nature*. 2011;473(7347):337-42.
  41. el Marjou F, Janssen KP, Chang BH, Li M, Hindie V, Chan L, Louvard D, Chambon P, Metzger D, and Robine S. Tissue-specific and inducible Cre-mediated recombination in the gut epithelium. *Genesis*. 2004;39(3):186-93.
  42. Luongo C, Moser AR, Gledhill S, and Dove WF. Loss of Apc<sup>+</sup> in intestinal adenomas from Min mice. *Cancer Res*. 1994;54(22):5947-52.
  43. Gao J, Aksoy BA, Dogrusoz U, Dresdner G, Gross B, Sumer SO, Sun Y, Jacobsen A, Sinha R, Larsson E, et al. Integrative analysis of complex cancer genomics and clinical profiles using the cBioPortal. *Sci Signal*. 2013;6(269):p11.
  44. Cerami E, Gao J, Dogrusoz U, Gross BE, Sumer SO, Aksoy BA, Jacobsen A, Byrne CJ, Heuer ML, Larsson E, et al. The cBio cancer genomics portal: an open platform for exploring multidimensional cancer genomics data. *Cancer Discov*. 2012;2(5):401-4.
  45. Giannakis M, Mu XJ, Shukla SA, Qian ZR, Cohen O, Nishihara R, Bahl S, Cao Y, Amin-Mansour A, Yamauchi M, et al. Genomic Correlates of Immune-Cell Infiltrates in Colorectal Carcinoma. *Cell Rep*. 2016;17(4):1206.



**Figure 1. *FBW7* is downregulated in human CRC.** (A) Representative images of RNAscope for *PPIB* and *FBW7*, and *FBW7* IHC on serial sections from human TMAs. u.d., undetected. Scale bar = 10  $\mu$ m. (B) Quantification of *FBW7* mRNA on colorectal cancer TMAs in 28 tissue cores positive for a control *PPIB* mRNA. (C) Quantification of *FBW7* IHC in tissue cores from A. (D–F) Endogenous *FBW7* interacts with endogenous USP9X and USP9X interacts with endogenous *FBW7* in HEK293 cells. Black line in D indicates noncontiguous lanes from the same gel. si-*FBW7* control in F confirms antibody specificity of *FBW7* and represents a negative control for *FBW7*-USP9X interaction. (G) Endogenous USP9X interacts with epitope-tagged *FBW7* isoforms  $\alpha$  and  $\beta$ .

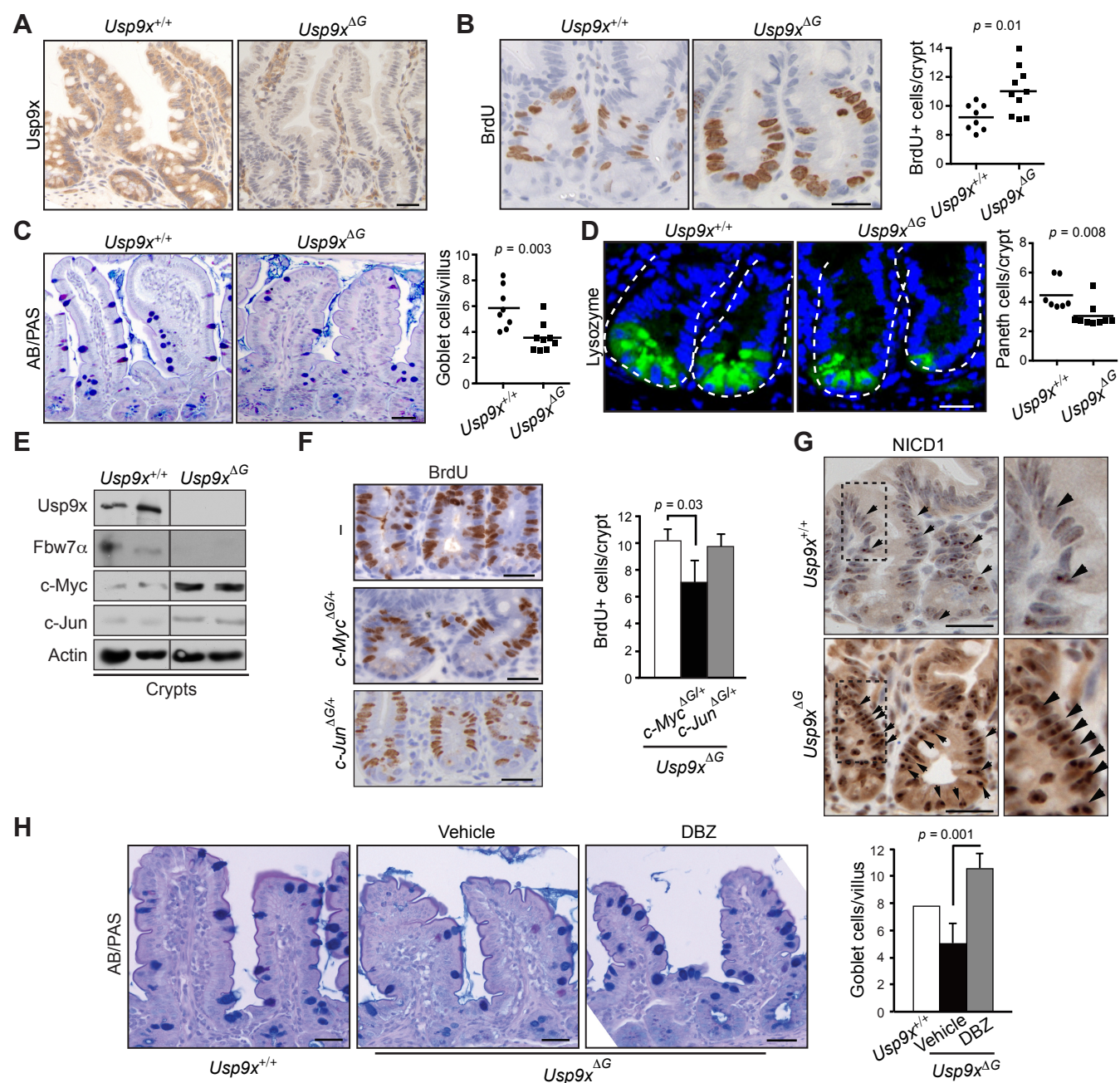


**Figure 2. FBW7 is a USP9X substrate.** (A and B) USP9X knockdown using multiple shRNAs reduced FBW7 protein levels with no effect on its mRNA. (C) MG132 rescues reduced FBW7 protein levels in USP9X silenced cells. (D) USP9X knockdown reduced the half-life of FBW7 protein. (E) Quantification of 3 independent experiments performed as in D. (F) Increased ubiquitylation of FBW7 in USP9X-silenced cells, UM = unmodified. (G) *In vitro* deubiquitylation of FBW7 by recombinant GST-USP9X, UM = unmodified. (H and I) Western blots for Flag-FBW7 $\alpha$  in HEK293 cells co-overexpressing wildtype (V5-Usp9x) or catalytically dead (V5-C1566S) mouse Usp9x. (J) Western blots on Ni-NTA pulldown samples from cells co-transfected with Flag-FBW7 $\alpha$  and the indicated constructs, UM = unmodified. All experiments were done in HEK293 cells.

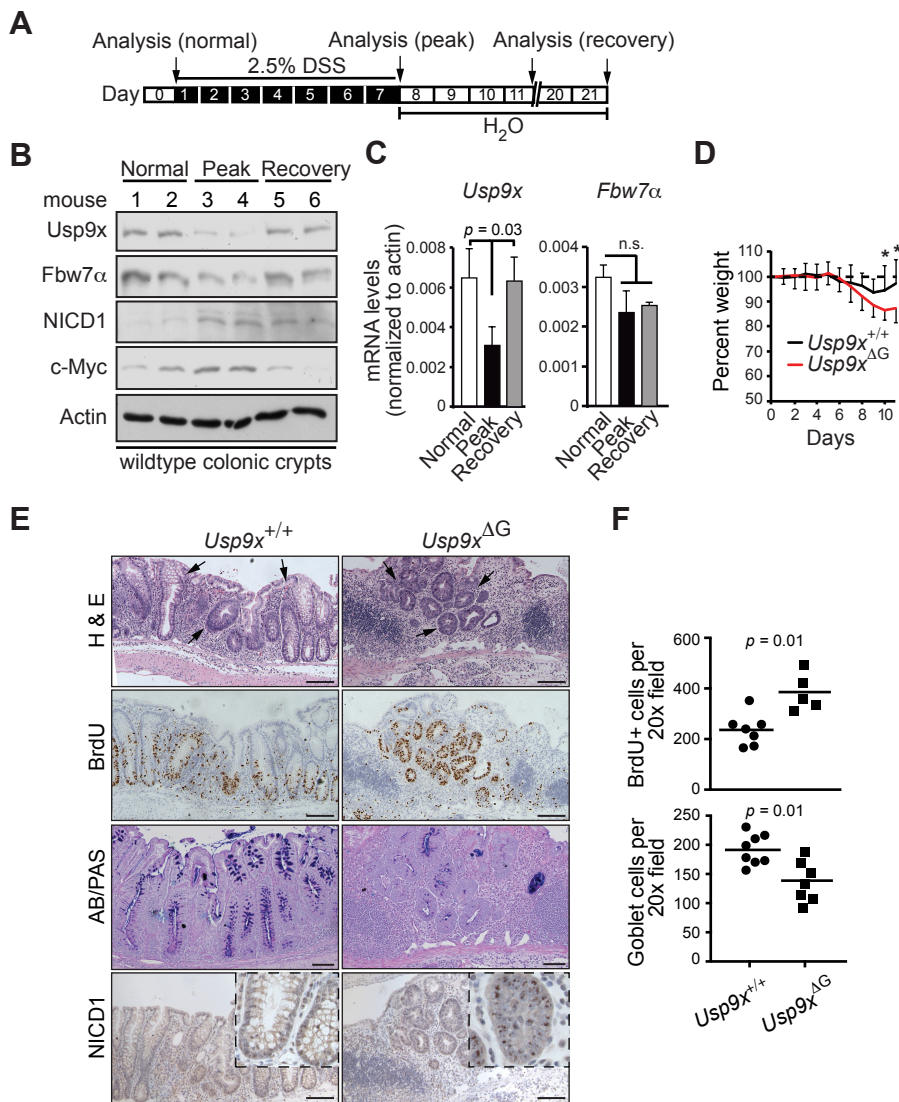


**Figure 3. USP9X negatively regulates SCF(FBW7) substrates.** (A) Accumulation of SCF(FBW7) substrates in *USP9X*-silenced HEK293 cells. (B) Accumulation of SCF(FBW7) substrates in *Usp9x*-knockout murine adult fibroblasts. (C) Western blots showing levels of SCF(FBW7) substrates in *USP9X*- and *ITCH*-silenced HEK293 cells. (D) Accumulation of SCF(FBW7) substrates with *USP9X* silencing was abolished in HCT116-*FBW7* <sup>$\Delta\Delta$</sup>  colorectal cancer cell line. (E and F) Western blots for ubiquitylated c-Myc on Ni-NTA pulldown from HEK293 cells overexpressing Flag-c-Myc and 6x-His-tagged ubiquitin and co-transfected with the indicated shRNAs. UM = unmodified. c-MYC mRNA levels in the same cells are shown in F. (G) c-MYC luciferase activity in HCT116 cells with indicated genotypes and siRNA treatments. Mean of 2 independent experiments shown.

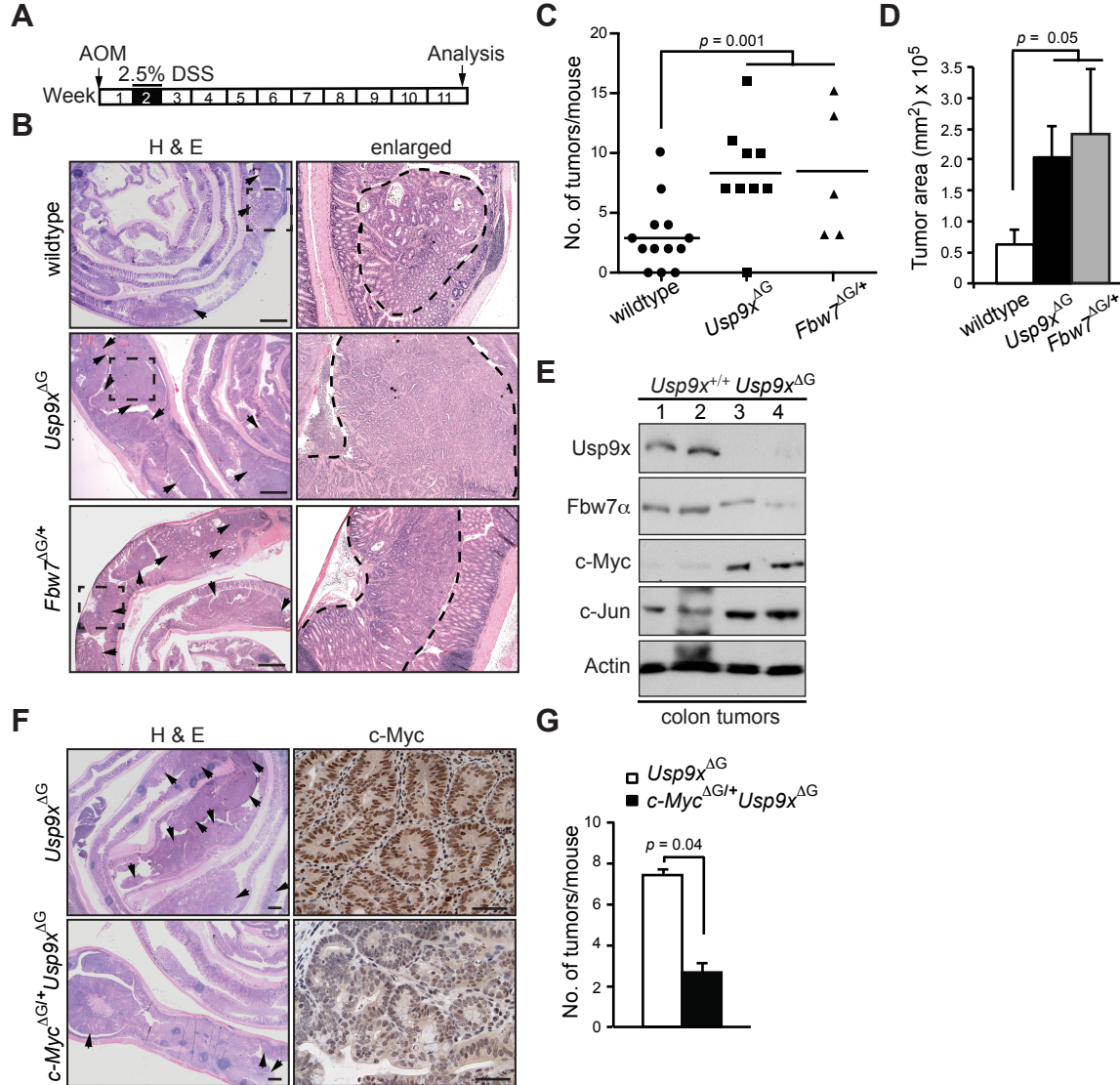




**Figure 4** *Usp9x* controls intestinal tissue homeostasis. (A, B, C, and D) Representative immunohistochemistry (IHC) sections for *Usp9x* (A), transit-amplifying cells (BrdU, B), goblet cells (AB/PAS, C), and Paneth cells (Lysozyme, D), in wildtype (*Usp9x*<sup>+/+</sup>) and *Usp9x*-knockout mouse gut. Scale bars = 50  $\mu$ m. Right panels, quantification from B–D,  $n = 5$ –8 mice/group. (E) Western blots for the indicated proteins in freshly isolated crypts from WT (wildtype) and *Usp9x*-knockout mouse gut. Black line indicates noncontiguous lanes from the same gel. (F) BrdU staining on gut cross sections from *Usp9x*<sup>ΔG/+</sup> mice. Right panel, quantification from F,  $n = 3$ –4 mice/group. (G) IHC for activated notch (NICD1) in mouse gut, scale bars = 50  $\mu$ m. (H) AB/PAS staining on guts from indicated mice treated with a vehicle or a notch inhibitor (DBZ), scale bars = 50  $\mu$ m. Right panel, quantification from H,  $n = 3$ –4 mice/group. Data are shown as mean + SD and statistical significance is calculated by student's t-test.

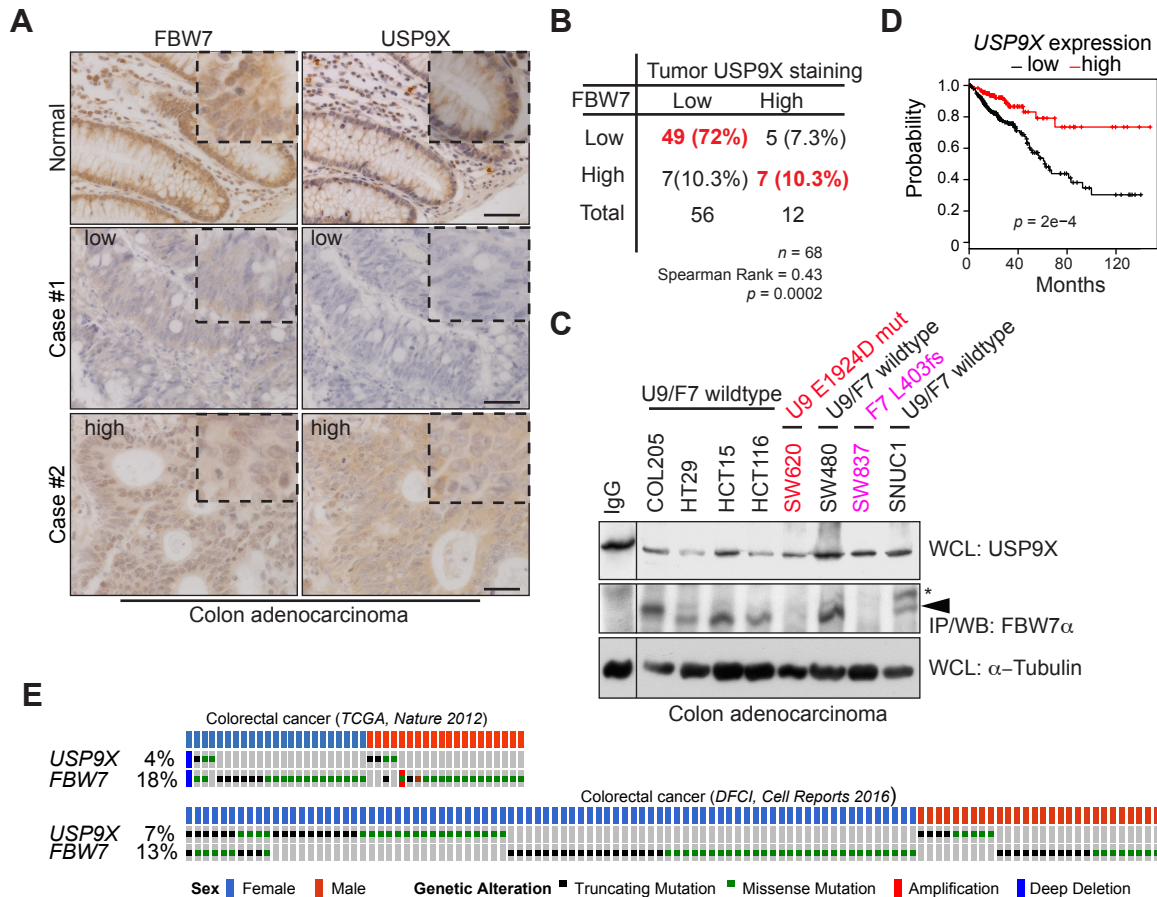


**Figure 5. *Usp9x* is required for tissue regeneration during acute colitis.** (A) Schematic of acute colitis protocol. (B) Western blots for the indicated proteins in six independent wildtype mice fed with (day 7, “peak” & day 21, “recovery”) or without (day 0, “normal”) 2.5 % DSS in water. (C) qRT-PCR analysis for *Usp9x* and *Fbw7* mRNA in different phases of colitis from experiment in B. Statistical significance calculated by one-way ANOVA. (D) Weight curves from DSS induced colitis experiment in indicated mice,  $n = 7-8/\text{group}$ . \* =  $p < 0.05$ . (E) Representative IHC sections for H&E, BrdU, AB/PAS and NICD1 from *Usp9x*<sup>+/+</sup> and *Usp9x* <sup>$\Delta$ G</sup> mice. Scale bars = 100  $\mu\text{m}$ . (F) Quantification of BrdU+ and AB/PAS+ cells from experiment in D. Data presented as mean, statistical significance calculated by student's t-test in D and F.



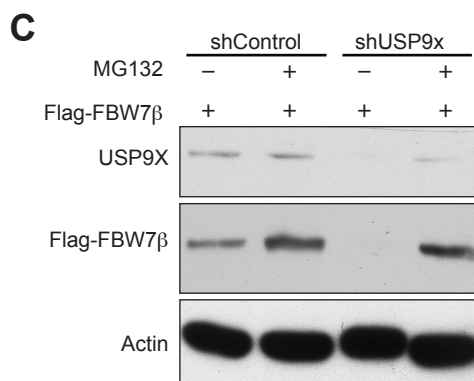
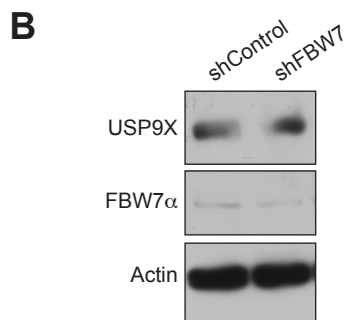
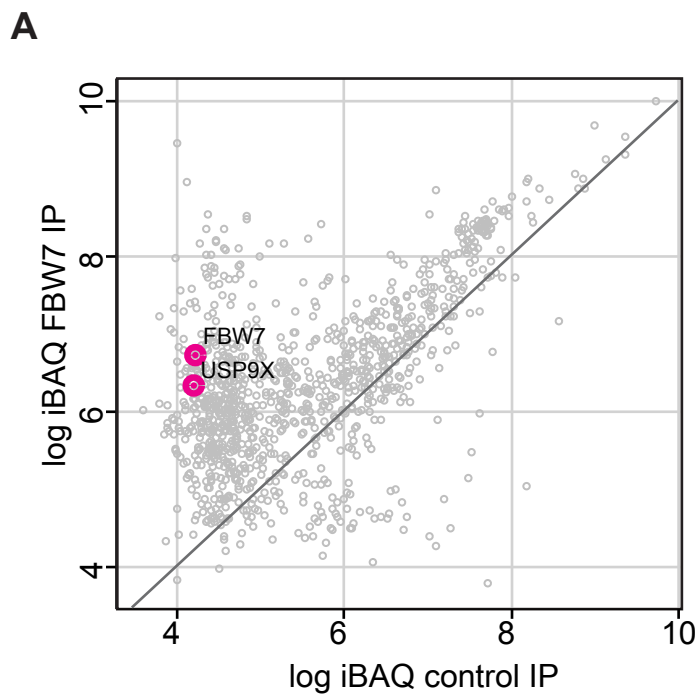
**Figure 6. *Usp9x* suppresses colorectal cancer.** (A) Schematic of AOM/DSS induced colorectal cancer model. (B) H&E on sections from transformed colons of the indicated genotypes. Scale bars = 100  $\mu$ m. (C) Number of tumors in each mouse from experiment in B,  $n = 5$ –13/group. (D) Tumor area represented as mm<sup>2</sup> in mice from B,  $n = 5$ –13/group. (E) Western blots showing levels of indicated proteins in four independent tumors from B. (F) H&E and c-Myc staining on sections from transformed colons of the indicated genotypes. Scale bars = 50  $\mu$ m. (G) Average number of tumors in indicated mice from experiment in F,  $n = 3$ –5/group. Data presented as mean, statistical significance calculated by one-way ANOVA in C and D, and by student's t-test in G.



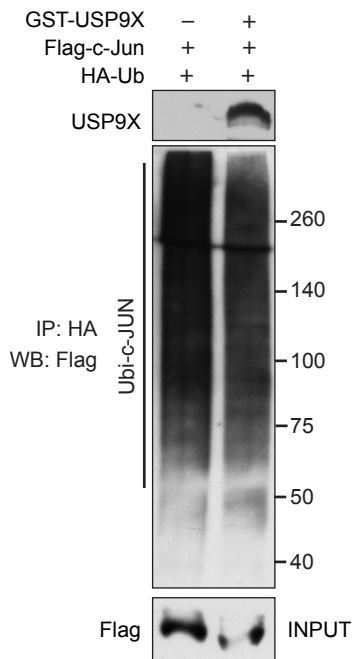
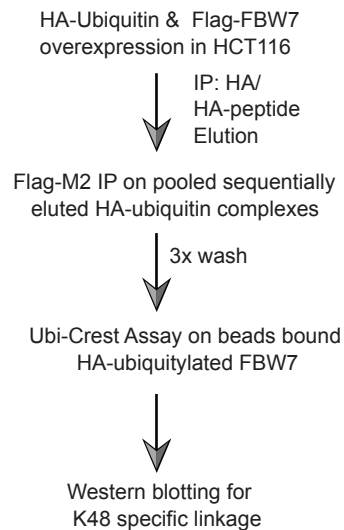
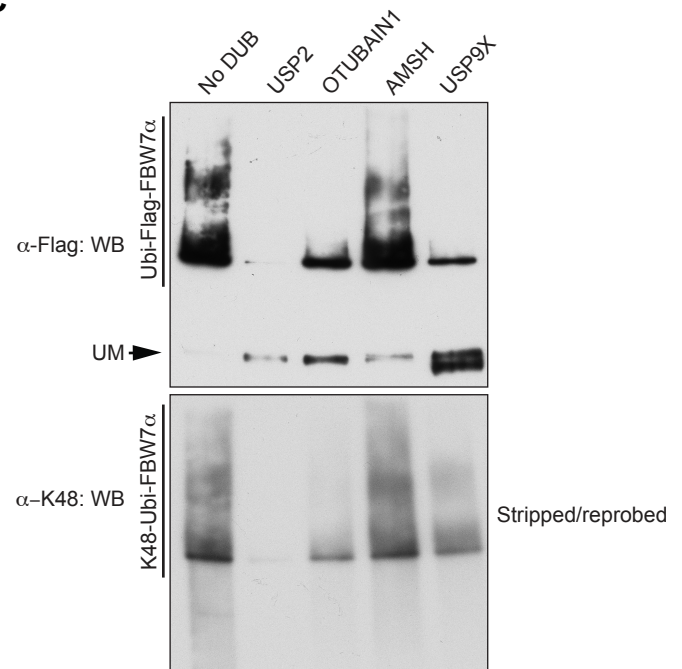


**Figure 7. Reduced USP9X is associated with poor prognosis in human colorectal cancer.** (A) IHC for the indicated proteins on human colorectal cancer tissue microarrays, including associated normal tissue. Scale bars = 50  $\mu$ m. (B) Quantification of staining intensities from sections in A, and their Spearman's rank correlation. (C) Western blots showing positive correlation of USP9X and FBW7 protein levels in 8 different colorectal cancer cell lines. Red = USP9X mutant, pink = FBW7 truncation mutant (homozygous) cell lines respectively. Black line indicates noncontiguous lanes from the same gel. (D) Kaplan-Meier plot showing comparison of survival between USP9X-low and -high expression groups of colorectal cancer patients. Data are from TCGA. (E) Mutational status of USP9X and FBW7 in CRC patients. Data are from the TCGA dataset of 212 patients and the DFC Colorectal Adenocarcinoma dataset of 619 patients published in refs<sup>(6, 45)</sup>. Data viewed with cBioPortal. Only samples with alterations in either USP9X or FBW7 are shown. Fisher's exact test  $p = 0.01$  for females and  $p = 1$  for males.



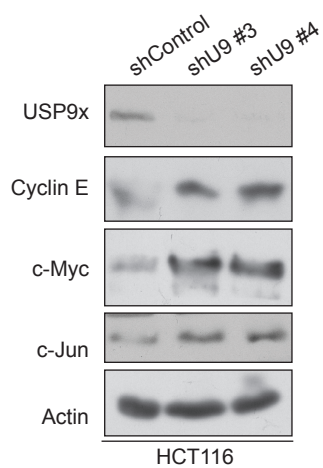


**Supplementary Figure 1. (A)** iBAQ plot showing MS-enrichment of FBW7 and interaction partners over a control IgG. **(B)** Western blots for indicated proteins in cells transfected with indicated shRNAs. **(C)** Western blots for indicated proteins in cells co-transfected with Flag-FBW7 $\beta$  and indicated shRNAs.

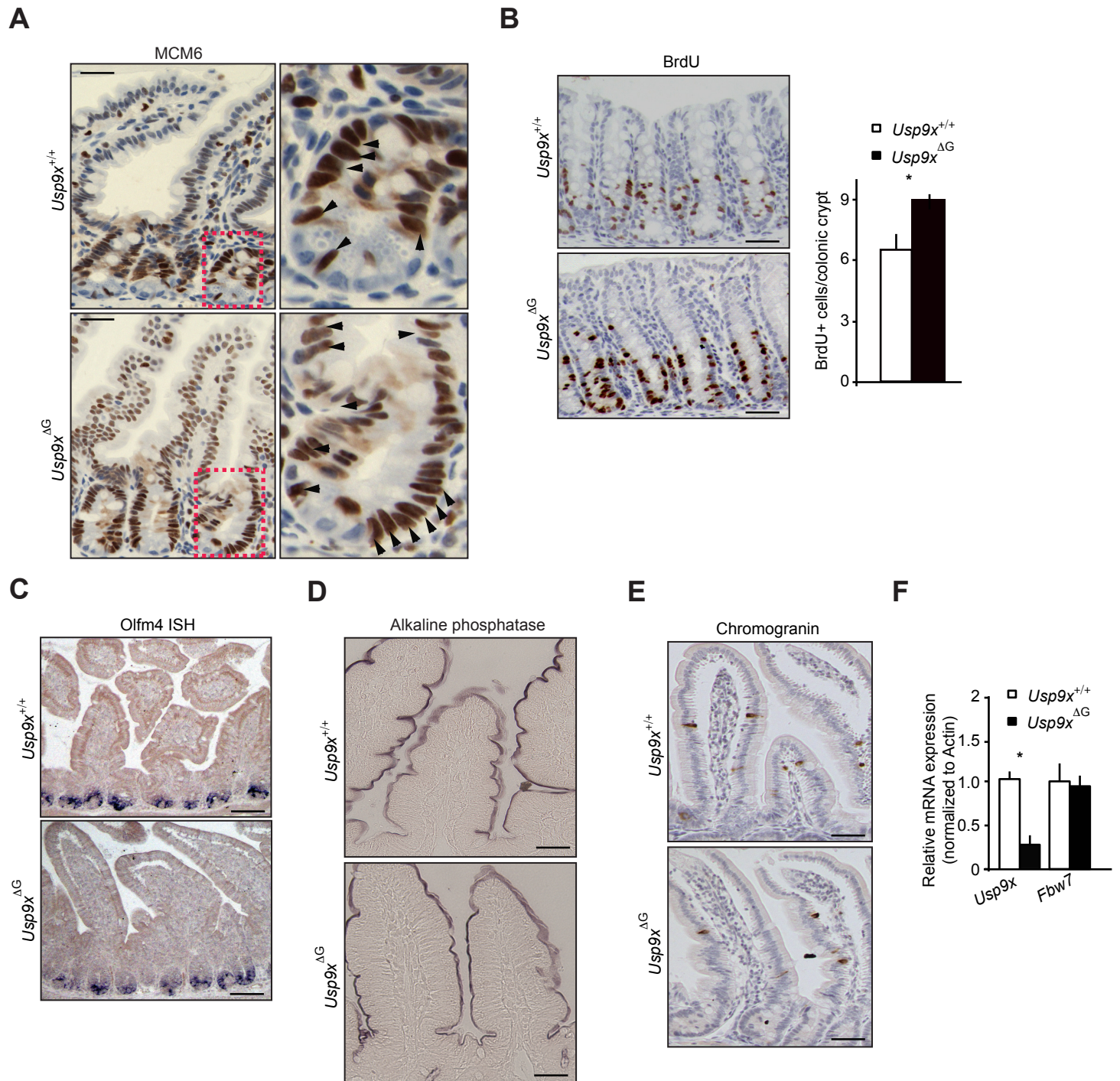
**A****B****C**

### Supplementary Figure 2. USP9X cleaves K48-linked polyubiquitin chains on FBW7.

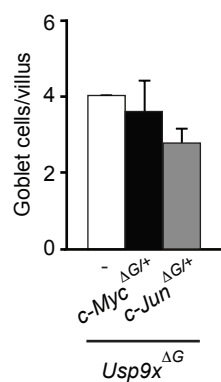
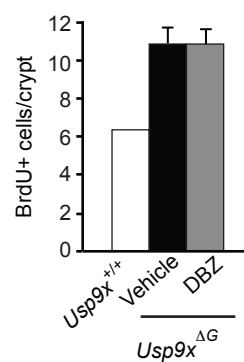
(A) Recombinant USP9X does not affect polyubiquitination of c-JUN in an in vitro deubiquitylation reaction. (B) Schematic for experiment in C. (C) Ubiquitin chain restriction (UbiCrest) experiment with indicated deubiquitinases: USP2 (promiscuous), OTUBAIN1 (K48-linked), and AMSH (K63-linked).



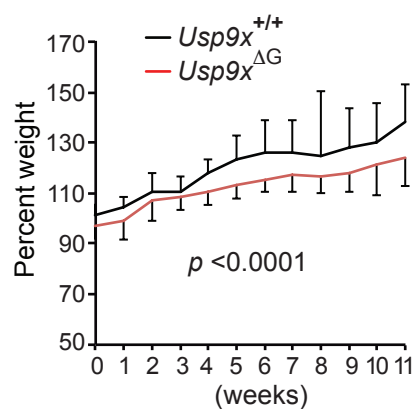
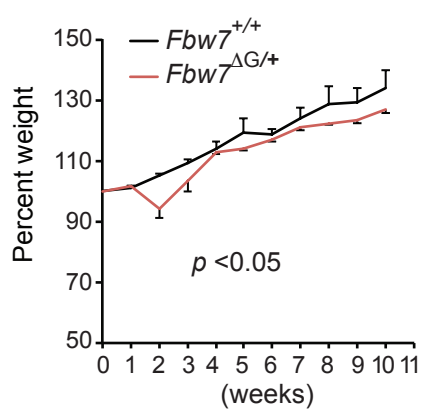
**Supplementary Figure 3.** Accumulation of SCF(FBW7) substrates in cells transfected with *USP9X*-shRNA compared to a non-targeting control.



**Supplementary Figure 4.** (A) IHC sections stained for proliferating cells (MCM6) from the intestine of indicated mice. Scale bar = 50  $\mu$ m. (B) BrdU staining for proliferating cells in colonic crypts from indicated mice, quantification shown in right panel. Scale bar = 100  $\mu$ m,  $n = 3-4$  mice/group. (C) *In situ* hybridization for *Olfm4* (stem cells) on the sections from the intestine of indicated mice. Scale bar = 100  $\mu$ m. (D and E) IHC for enterocytes (Alkaline phosphatase) and enteroendocrine cells (Chromogranin) in gut from indicated mice. Scale bars = 100  $\mu$ m. (F) qRT-PCR analysis showing mRNA levels of indicated genes normalised to actin and represented as fold change over control, in isolated crypts from  $Usp9x^{+/+}$  (wildtype) and  $Usp9x^{\Delta G}$  gut,  $n = 5-8$  mice/group.

**A****B**

**Supplementary Figure 5. (A)** Average goblet cell number per villus from indicated mice. **(B)** Average BrdU+ cell number per crypt from indicated mice.

**A****B**

**Supplementary Figure 6.** (A and B) Weight curves presented as percent of starting weight in indicated mice from colitis-driven tumorigenesis experiment,  $n = 5-9$  animals/genotype.  $P$  values were calculated by Log-rank (Mantel-Cox) test.

**Supplementary Table.** Shortlisted candidates from IP-mass spectrometry experiment using endogenous FBW7 as bait.

Gene Symbol	Description	Function
<b>FBXW7</b>	<b>F-box/WD repeat-containing protein 7</b>	<b>E3 Ligase</b>
<b>SKP1</b>	<b>S-phase kinase-associated protein 1</b>	<b>SCF Component</b>
UBAP2L	Ubiquitin-associated protein 2-like	Ubiquitylation
MYCBP2	MYC binding protein 2	Probable E3 ubiquitin-protein ligase
HERC2	E3 ubiquitin-protein ligase HERC2	E3 Ligase
HUWE1	E3 ubiquitin-protein ligase HUWE1	E3 Ligase
HECTD1	E3 ubiquitin-protein ligase HECTD1	E3 Ligase
<b>USP9X</b>	<b>Probable ubiquitin carboxyl-terminal hydrolase FAF-X</b>	<b>Deubiquitinase</b>
USP20	Ubiquitin carboxyl-terminal hydrolase 20	Deubiquitinase
FKBP8	Peptidyl-prolyl cis-trans isomerase FKBP8	Chaperon
FKBP4	Peptidyl-prolyl cis-trans isomerase FKBP4	Chaperon
PSMA2	Proteasome subunit alpha type-2	Proteasome subunit
PSMA3	Proteasome subunit alpha type-3	Proteasome subunit
PSMA6	Proteasome subunit alpha type	Proteasome subunit
PSMD3	26S proteasome non-ATPase regulatory subunit 3	Proteasome subunit
FOXP2	Forkhead box protein P2	Transcription factor
c-JUN	Transcription factor AP-1	Transcription factor
STAT1	Signal transducer and activator of transcription 1-alpha/beta	Transcription factor
MSH6	DNA mismatch repair protein Msh6	DNA replication/Genome integrity
MCM3	DNA replication licensing factor MCM3	DNA replication/Genome integrity
MCM7	DNA replication licensing factor MCM7	DNA replication/Genome integrity
TOP1	DNA topoisomerase 1	DNA replication/Genome integrity
RAD21	Double-strand-break repair protein rad21 homolog	DNA replication/Genome integrity
NAP1L1	Nucleosome assembly protein 1-like 1	DNA replication/Genome integrity
HDAC2	Histone deacetylase 2;Histone deacetylase	DNA replication/Genome integrity
CHD4	Chromodomain-helicase-DNA-binding protein 4	DNA replication/Genome integrity
MRE11A	Double-strand break repair protein MRE11A	DNA replication/Genome integrity
DNAJB6	DnaJ homolog subfamily B member 6	DNA replication/Genome integrity
MTOR	Serine/threonine-protein kinase mTOR	Kinase
STK3	Serine/threonine-protein kinase 3	Kinase
PANK2	Pantothenate kinase 2, mitochondrial	Kinase
GALK1	Galactokinase	Kinase
DEK	Protein DEK	Kinase
CSNK1A1	Casein kinase I isoform alpha	Kinase
PI4KB	Phosphatidylinositol 4-kinase beta	Kinase
WEE1	Wee1-like protein kinase	Kinase
XPO1	Exportin-1	Nuclear export
CSE1L	Exportin-2	Nuclear export
KPNB1	Importin subunit beta-1	Nuclear import
RANBP1	Ran-specific GTPase-activating protein	Transport
LUC7L	Putative RNA-binding protein Luc7-like 1	RNA binding/processing

DDX39	ATP-dependent RNA helicase DDX39A	RNA binding/processing
MARS	Methionine-tRNA ligase, cytoplasmic	RNA binding/processing
RAE1	mRNA export factor	RNA binding/processing
BCAS2	Pre-mRNA-splicing factor SPF27	RNA binding/processing
LARS	Leucine--tRNA ligase, cytoplasmic	RNA binding/processing
RBM39	RNA-binding protein 39	RNA binding/processing
RBM28	RNA-binding protein 28	RNA binding/processing
DDX24	ATP-dependent RNA helicase DDX24	RNA binding/processing
TARS	Threonine--tRNA ligase, cytoplasmic	RNA binding/processing
FMR1	Fragile X mental retardation protein 1	RNA binding/processing
IARS	Isoleucine--tRNA ligase, cytoplasmic	RNA binding/processing
YBX2	DNA-binding protein A;Y-box-binding protein 2	RNA binding/processing
MLL	Histone-lysine N-methyltransferase	Enzyme
RPN2	DPD glycosyltransferase subunit 2	Enzyme
DPM1	Dolichol-phosphate mannosyltransferase	Enzyme
PRMT1	Protein arginine N-methyltransferase 1	Enzyme
ACLY	ATP-citrate synthase	Enzyme
EIF4G1	Eukaryotic translation initiation factor 4 gamma 1	Translation
EIF3F	Eukaryotic translation initiation factor 3 subunit F	Translation
EIF2B4	Translation initiation factor eIF-2B subunit delta	Translation
EIF5B	Eukaryotic translation initiation factor 5B	Translation
MFF	Mitochondrial fission factor	Mitochondrial
SSBP1	Single-stranded DNA-binding protein, mitochondrial	Mitochondrial
ATP5J2	ATP synthase subunit f, mitochondrial	Mitochondrial
MTCH2	Mitochondrial carrier homolog 2	Mitochondrial
MAGED2	Melanoma-associated antigen D2	Cell adhesion
ACTR2	Actin-related protein 2	Cytoskeleton
TUBA1C	Tubulin alpha-1C chain	Cytoskeleton
TUBB2A	Tubulin beta-2A chain	Cytoskeleton